William & Mary
CHARTERED 1693

W&M ScholarWorks

Dissertations, Theses, and Masters Projects

Theses, Dissertations, & Master Projects

2024

Projected Impacts Of Climate Change And Watershed Management On Carbonate Chemistry And Oyster Growth In A Coastal Plain Estuary

Catherine Czajka
William & Mary - Virginia Institute of Marine Science, czajkacatherine@gmail.com

Follow this and additional works at: https://scholarworks.wm.edu/etd

 Part of the Oceanography Commons

Recommended Citation

Czajka, Catherine, "Projected Impacts Of Climate Change And Watershed Management On Carbonate Chemistry And Oyster Growth In A Coastal Plain Estuary" (2024). *Dissertations, Theses, and Masters Projects.* William & Mary. Paper 1717521754.
https://dx.doi.org/10.25773/v5-rn0n-ff21

This Thesis is brought to you for free and open access by the Theses, Dissertations, & Master Projects at W&M ScholarWorks. It has been accepted for inclusion in Dissertations, Theses, and Masters Projects by an authorized administrator of W&M ScholarWorks. For more information, please contact scholarworks@wm.edu.

Projected impacts of climate change and watershed management on carbonate chemistry and oyster growth in a coastal plain estuary

A Thesis

Presented to

The Faculty of the School of Marine Science

The College of William and Mary in Virginia

In Partial Fulfillment

of the Requirements for the Degree of

Master of Science

by

Catherine Czajka

May 2024

© Copyright by Catherine Czajka 2024

APPROVAL PAGE

This thesis is submitted in partial fulfillment of

the requirements for the degree of

Master of Science

Catherine Czajka

Approved by the Committee, May 2024

Marjorie A.M. Friedrichs, Ph.D.
Committee Chair / Advisor

Emily B. Rivest, Ph.D.
Co-Advisor

Pierre St-Laurent, Ph.D.

Mark Brush, Ph.D.

William Walton, Ph.D.

TABLE OF CONTENTS

ACKNOWLEDGEMENTS

This thesis would never have been completed without the unwavering support of so many people. First and foremost, thank you to both of my advisors, Dr. Marjy Friedrichs and Dr. Emily Rivest. You both go above and beyond to support your students, and I don't know when you sleep! Both of you have been so supportive of my research and professional goals, and have offered so much valuable feedback and guidance over the years. Thank you for providing such consistent advisement and support and for making me a better scientist.

I would like to extend my sincere gratitude to all of my (many) lab mates that I have had over the past two and a half years. We have spent countless hours together in lab meetings or practice presentations, and I am certain the quality of my work would be lesser without you all. I am fortunate to have had lab mates who are so generous with their time and knowledge. Thank you to Fei Da and Kyle Hinson for being invaluable in teaching me the ropes of ROMS and navigating my early life at VIMS. Thank you to Colin Hawes for being an amazing sidekick to enter into the world of modeling with. Thank you to Abbey Sisti for being an incredible office mate, better travel buddy, and even better personal photographer. Additionally, thank you to Annie Schatz, Taylor Walker, Anthony Himes, Alexa Labossiere, Olivia Szot, Dante Horemens, Brandylyn Thomas, Javier Pujols, Alexis Putney and Margaret O'Connor for your camaraderie, feedback, and help over the years.

I would also like to thank the members of the STAR project for their excellent feedback and interesting collaboration over the past several years. Specifically, I'd like to thank Sara Blachman for all of her hard work on the EcoOyster model and Brian Katz for his consistently helpful advice.

Additionally, thank you to my committee members, Dr. Pierre St-Laurent, Dr. Mark Brush, and Dr. Bill Walton, for your support and stimulating conversations. Without you all this project would be far inferior. Pierre, you have been a lifesaver more times than I can count. Thank you for being such a great person to bounce ideas off of and sharing a slice of your modeling genius.

Most importantly, thank you to my family for all of your support over the years. Both my immediate family, and my VIMS family that I am very fortunate to have. I have made lifelong friendships and precious memories at VIMS that I cherish so deeply. You all are hilarious and make every day fun, and I am grateful for you all the time. In particular, I want to thank Sarah Koshak, and Ben and Tiny, for bringing me into your Mercer Rd family unit in more ways than one. Best roommates ever. And of course, thank you to the rest of my lemon gang: Matt LaGanke, Evan Hill, and the very important honorary member, Mary Bryan Barksdale. You know why ☺

This project was funded by the NOAA Ocean Acidification Program. Thank you for the financial support, and for giving me the opportunity to attend meetings in Peru and San Diego, where I learned so much about this field and got to play a small part in the process of directing scientific research with real-world impacts.

ABSTRACT

Coastal acidification, warming, and nutrient management actions all alter water quality conditions that marine species experience, with potential impacts to their physiological processes. Decreases in calcite saturation state (Ω_{Ca}) and food availability, combined with warming water temperatures, pose a threat to calcifying organisms; however, the magnitude of future changes in estuarine systems is challenging to predict and not well known. This study aims to determine how and where oysters will be affected by future acidification, warming, and nutrient reductions, and the relative effects of these stressors. To address these goals, an oyster bioenergetics model for Eastern oysters (*Crassostrea virginica*) was embedded in a 3-D coupled hydrodynamic-biogeochemistry model implemented for tributaries in the lower Chesapeake Bay. Model simulations were forced with projected future conditions (mid-21st century atmospheric CO_2, atmospheric temperature, and managed nutrient reductions) and compared with a realistic present-day reference run. Together, all three stressors are projected to reduce Ω_{Ca} and growth of oyster shell and tissue. Increased atmospheric CO_2 and temperature are both projected to cause widespread reductions in $\Omega_{Ca.}$ The resulting reductions in oyster shell and tissue growth will be most severe along the tributary shoals. Future warming during peak oyster growing seasons is projected to have the strongest negative influence on tissue and shell growth, due to summer water temperatures reducing filtration rates, enhancing respiration and shell dissolution rates, and increasing organic matter remineralization rates, thus reducing food availability. Nutrient reductions will exacerbate deficits in oyster food availability, contributing to further reductions in growth. Quantifying the effects of these stressors provides insight on the areas in the lower bay where oysters will be most vulnerable to mid 21st-century conditions.

Projected impacts of climate change and watershed management on carbonate chemistry and oyster growth in a coastal plain estuary

1. Introduction

Anthropogenic climate change and its associated impacts on water quality may threaten marine organisms and economic systems reliant on them. Oceanic uptake of increasing anthropogenic atmospheric carbon dioxide (CO_2) causes a decrease in seawater pH and saturation states of calcium carbonate, a phenomenon known as ocean acidification (Caldeira and Wickett, 2003; Doney et al., 2009). Globally, the ocean has absorbed about 30% of anthropogenic atmospheric CO_2 since pre-industrial times (Gruber et al., 2019), and open-ocean surface pH is anticipated to decrease by 0.3 units on average by the end of the century under 'business-as-usual' conditions (Riahi et al., 2011; IPCC, 2019). The percent volume of ocean water undersaturated with calcite ($\Omega_{Ca} < 1$) is predicted to expand to 91% by 2100 from 76% in the 1990s (Caldeira and Wicket, 2005; Gattuso et al., 2015).

Since estuaries have lower and more variable pH than the open-ocean, the effects of increased atmospheric CO_2 on estuarine water quality and biota are often amplified. In coastal and estuarine systems, acidification may be exacerbated by local-level processes, such as the input of acidic freshwater and nutrient runoff from precipitation, a process termed coastal acidification (Salisbury et al., 2008; Wallace et al., 2014; Cartensen and Duarte 2019). Freshwater has relatively low total alkalinity (TA), or buffering capacity, so areas in estuaries with greater relative freshwater influence cannot resist changes to pH as easily as more saline or open-ocean waters (Hasler et al., 2018). Eutrophication, the increased rate of organic matter input to a system (Nixon 1995), may drive large variations in local pH and overall water quality. Elevated nutrient inputs cause pH to increase in surface waters due to higher primary productivity, which will reduce surface acidification; however, pH will decrease in deeper bottom waters as the additional organic matter sinks and is remineralized (Cai et al., 2021). Management actions to reduce eutrophication

and improve water quality in bottom waters have been successful but may also enhance acidification in shallow surface waters by lowering primary productivity (Borges and Gypens, 2010). The overall effect of future changes in nutrient inputs on coastal biogeochemistry is thus unclear.

Warming, another driver of biogeochemical change in coastal waters, may compound or offset the effects of increased atmospheric CO_2 on coastal ecosystems. The global ocean has absorbed approximately 93% of the atmospheric heat produced by anthropogenic activity, leading to a global sea surface temperature increase of 0.7°C since 1900 (Jewett and Romanou, 2017). Ocean warming is expected to continue, with global averages increasing by 2.7°C by 2100 and greater increases expected in shallow coastal regions (Jewett and Romanou, 2017). Coastal acidification may accelerate as warming of coastal waters increases rates of biogeochemical processes; increased respiration rates may drive larger diel variations in pH, dissolved oxygen, and associated water quality (Du et al., 2018; Tian et al., 2021). Therefore, it is vital to understand how warming will interact with acidification to predict local changes in water quality and health of coastal organisms.

Characterizing spatiotemporal patterns of acidification in estuarine waters is important, as negative impacts of acidification on the biology of marine organisms may be substantial. Acidification disrupts the formation of calcium carbonate ($CaCO_3$) during shell-building, i.e., biocalcification, which is a vital process for growth and survival of many aquatic invertebrate species (e.g., Orr et al., 2005; Gazeau et al., 2007; Dong et al., 2023). Under acidified conditions, water concentrations of CO_2 and H^+ increase, and concentrations of carbonate ions ($[CO_3^{2-}]$) decrease. A low ambient $[CO_3^{2-}]$ inhibits calcifying organisms from forming $CaCO_3$ for their shells, as more energy is required to precipitate CO_3^{2-} from acidified waters (e.g., Guinotte and

Fabry 2008; Lutier et al., 2022; Matoo et al., 2020; Mederios & Souza 2023). Low Ω_{Ca} may also lead to net dissolution of $CaCO_3$, leading to weaker shells and greater juvenile susceptibility to predation (e.g., Waldbusser et al., 2011; Amaral et al., 2012; Barclay et al., 2020). Acidification may further reduce shell growth through adverse physiological effects that limit energy availability for calcification. Because acidification is often more extreme in estuaries, oysters and other commercially valuable coastal bivalve species experience stronger effects of climate change than organisms living in open-ocean environments (Poach et al., 2019; Melzner et al., 2020; Cai et al., 2021). Prior experiments have revealed negative effects of acidification, warming, and nutrient reductions on oyster biocalcification and growth (Beniash et al., 2010; Waldbusser et al., 2011; Gobler and Talmage, 2014), but it is yet to be determined how the impacts of these stressors on oyster shell and tissue growth will vary spatially in highly dynamic systems.

The Chesapeake Bay is an excellent study system for examining the interacting influences of acidification, warming, and nutrient reductions (hereafter referred to collectively as "future stressors") on estuarine biogeochemistry and the organisms living there. The bay exhibits high temporal and spatial variability in pH due to seasonal phytoplankton blooms, eutrophication, and acidic freshwater input (Da et al., 2021; St-Laurent et al., 2020; Kemp et al., 2005; Cai et al., 2021). From the mid-1980s to mid-2010s, surface waters in the upper bay experienced pH increases between +0.2 and +0.4 pH units in early spring and fall due to increased riverine TA from lowered nitrate inputs, while surface waters in the nitrogen-limited middle bay decreased up to -0.24 pH units during late spring and summer as a result of decreased primary production (Da et al., 2021). Over the same time period, the bay warmed by 0.24 ± 0.15°C per decade (Hinson et al., 2022), more than double the average rate of warming for the upper 75m of the global ocean (Rhein et al., 2013). Warming has also led to more severe hypoxia (Irby et al., 2018; Ni et al., 2020; Frankel et

al., 2023; Hinson et al., 2023). In 2010, the Environmental Protection Agency mandated a Total Maximum Daily Load (TMDL) of pollutants from point and non-point sources to be achieved by 2025 (EPA, 2010). As nutrient reductions negatively affect pH in surface waters of the bay (Shen et al., 2020; Da et al., 2021), achieving the TMDLs may actually worsen acidification in shallow and near-shore regions. Much of the research effort devoted to characterizing present-day carbonate chemistry and its historical trends has focused on the mainstem and upper Chesapeake Bay (Cai et al., 2017; Shen et al., 2020, Su et al., 2020), and less is known about these conditions throughout the tributaries of the lower bay (Shadwick et al., 2019).

The combined effects of future stressors will impact calcifying organisms in the lower Chesapeake Bay as well as the economic systems reliant upon them. The Eastern oyster *Crassostrea virginica* (Gmelin, 1791) is a foundation species native to the bay (Dayton, 1972). Eastern oyster aquaculture in this region has grown rapidly in the past few decades, with Virginia becoming the third most productive oyster fishery in 2018 (Hudson, 2019), largely a result of the development of disease-resistant oyster strains (Frank-Lawale et al., 2014). Negative impacts of acidification on aquaculture practices in other parts of the world (Barton et al., 2015) have already stirred concern over the vulnerability of oysters in the Chesapeake Bay. For example, in the Pacific Northwest, major larval mortality occurred at a shellfish hatchery following an upwelling event that lowered pH and Ω of aragonite, which had cascading impacts on the oyster industry all along the West Coast (Barton et al., 2015). While most effects of acidification on aquaculture have been observed in oyster larvae in hatcheries, fewer studies have examined acidification's influence on adult oysters when deployed in the field. To support the future of the oyster aquaculture industry in Chesapeake Bay, it is critical to identify which areas in the bay will be most vulnerable to

acidification at mid-century and how each driver of change contributes to acidification and its impacts on growth.

This study addresses the following primary research question: How and where will carbonate chemistry and Eastern oyster growth in the lower Chesapeake Bay change in the future and which future stressors will drive these changes? A three-dimensional hydrodynamic-biogeochemical model is coupled with an oyster bioenergetics model and is applied to two major Virginia tributaries of the Chesapeake Bay. The model provides detailed information on present-day environmental conditions, and when combined with climate projections from Earth System Models, allows for simulations of the independent and interacting influences of future environmental change on carbonate chemistry and Eastern oysters. This study provides insight into which areas are most vulnerable to mid 21st-century acidification and how acidification, warming, and nutrient loading may each impact oyster growth in isolation as well as via simultaneous co-stressors.

2. Methods

2.1 Model description

2.1.1 Hydrodynamic model

This study uses the three-dimensional hydrodynamic Regional Ocean Modeling System (ROMS; Shchepetkin and McWilliams, 2005), implemented similarly to St-Laurent and Friedrichs (2024) but on a higher resolution grid focused on two of the lower Virginia Chesapeake Bay tributaries (Fig. 1). The model domain (Da, 2023) includes the York and Rappahannock Rivers, as well as a portion of the mainstem shoal north of the Rappahannock. The model grid consists of 620x740 horizontal grid cells with a horizontal resolution of 120 m, allowing for greater resolution

of coastlines than many other Chesapeake Bay model grids (Irby et al., 2016). The hydrodynamic model includes 20 terrain-following vertical levels and two primary state variables: practical salinity and potential temperature. A wetting and drying scheme has been implemented to represent water levels and currents in coastal grid cells (Warner et al., 2013; St-Laurent and Friedrichs, 2024).

2.1.2 Carbon and biogeochemistry model

The Estuarine-Carbon-Biogeochemistry model (ECB) embedded in ROMS and used in this study has previously been implemented in the Chesapeake Bay (Feng et al., 2015; St-Laurent et al., 2020; Frankel et al., 2022; Hinson et al., 2023) as well as in the lower Virginia tributaries (Da, 2023). ECB simulates full carbon and nitrogen cycles of the lower trophic levels, represented by the following state variables: nitrate, ammonium, phytoplankton and zooplankton nitrogen, small and large detrital nitrogen and carbon, semi-labile and refractory dissolved organic nitrogen, DIC, TA, and dissolved oxygen (O_2). Phytoplankton and zooplankton carbon and dissolved organic carbon (DOC) are calculated from established C:N ratios (Redfield, 1934; Hopkinson et al., 1998). Biogeochemical processes include primary production, aggregation, sinking, basal metabolism, exudation, sloppy feeding, excretion, metabolism, nitrification/denitrification, remineralization, grazing, and mortality. Additional biogeochemical sources and sinks are included in the bottom vertical level (e.g., burial, resuspension, nitrification/denitrification, remineralization, sediment O_2 and CO_2 exchange). Light attenuation throughout the water column is based on the diffuse attenuation coefficient (Kd), which is parameterized as a function of surface TSS (including inorganic and organic components) and salinity as a proxy for colored dissolved organic matter (Feng et al., 2015; Turner et al., 2021). The sediment transport module within ECB is comprised

of two vertical seabed layers that simulate four suspended sediment size classes (Turner et al., 2021).

The carbon module within ECB has been fine-tuned in this implementation of the model, allowing for greater performance in acidification simulations (Da, 2023). The model grid includes tidal wetlands along the York River based on estimated wetland areas (Mitchell et al., 2017), which further contribute to TA fluxes through sulfate reduction in sediments (Raymond et al., 2000; Najjar et al., 2020). Ω_{Ca} is calculated from DIC, TA, temperature, and salinity using CO2SYS (van Heuven et al., 2011) using the equilibrium constants of Cai and Wang (1998) as in Da (2023). Although submerged aquatic vegetation is a possible source of $CaCO_3$ (Mazarrasa et al., 2015; Su et al., 2020), $CaCO_3$ precipitation and dissolution are not simulated in ECB due to both insufficient observations and low submerged aquatic vegetation presence throughout the model domain (Orth et al., 1998; Moore et al., 2009).

Several updates have been made in this implementation of ROMS-ECB to better represent oxygen and primary production dynamics in the lower Virginia tributaries. The minimum phytoplankton growth rate has been increased to 2.15 d^{-1}, and the growth rate is limited in the fresh portion of the tributaries using a Michaelis-Menten function of salinity and a half-saturation of 1.5 (Da, 2023). Sediment oxygen demand is included at the wetlands bottom boundary to simulate the aerobic processes occurring in the sediments (Da, 2023). The sediment bed climatology from Moriarty et al. (2021) has been adjusted to better represent the sand class distributions published in Nichols (1991) and observations taken by the USGS (Reid et al., 2005). Specifically, the changes include a greater percentage of small clay-rich flocs throughout the main stem of the York River as well as more sand and large silt-rich flocs in the Rappahannock River. Previously, the sediment module assumed the same critical shear stress for large silt-rich flocs, small clay-rich

flocs, and unaggregated mud; here, the critical shear stress of smaller particles is lower than larger particles, meaning smaller particles resuspend more easily. The updated critical shear stress coefficient for erosion and deposition is 0.5 Pa for large silt-rich flocs and 0.4 Pa for both small clay-rich flocs and unaggregated mud, which represent a small portion of the sediment bed. The ballasting formulation of Turner et al. (2021) has also been added to simulate the increase in particle sinking rates due to the aggregation of particles in turbid waters.

2.1.3 Oyster bioenergetics model

As part of this study, the oyster bioenergetics model EcoOyster (Brush and Kellogg, 2018; Kellogg et al., 2018) has been one-way coupled to ROMS-ECB in the deepest (bottom) level (see Supplementary Tables S1-S4 for EcoOyster equations). The coupled model, referred to hereafter as ROMS-ECBO, simulates daily somatic tissue weight, gonadal tissue weight, shell weight, and shell height of diploid oysters as a function of filtration, respiration, egestion, allocation to reproduction, calcification, and dissolution (Brush et al., 2024). Tissue growth rates depend on temperature, salinity, dissolved oxygen, total suspended solids (TSS), and particulate organic carbon (POC) from ROMS-ECB. Chl*a* is required for the filtration function and is calculated from ROMS-ECB phytoplankton carbon and Kd, in combination with seasonal carbon:chl*a* ratios that are computed using equations from Cerco and Noel (2004). The calcification function includes a threshold value of $\Omega_{Ca} = 0.93$, determined through laboratory experiments with Eastern oysters (Rivest et al., 2023).

The EcoOyster equations are developed from a meta-analysis of existing oyster bioenergetics models and laboratory experiments with diploid oysters (Rivest et al., 2023). Allometric relationships between shell weight, tissue weight, and shell height used for initial conditions are derived from observational data in the Chesapeake Bay (VOSARA, 2024). Total

dry tissue weight is calculated as the sum of somatic tissue weight and gonadal weight. Reproduction is simulated through gonadal weight, a function of growth of gonadal tissue, resorption of gonadal tissue, and spawning (Hofmann et al., 1994). Somatic tissue weight is a function of assimilation, respiration, growth of gonadal tissue, and resorption of gonadal tissue. Assimilation is a function of filtration and POC. Filtration is a function of limiting temperature, salinity, TSS, O_2, and chl*a,* and a maximum filtration rate based on tissue weight (Cerco and Noel 2005; Fulford et al., 2007; Ehrich and Harris 2015). The optimal temperature for oyster filtration (T_{opt}) is set to 27 °C (Jordan, 1987). Filtration is also multiplied by *p*, a tunable factor to better simulate time spent filtering based on published growth rates. Respiration is a function of tissue weight, temperature, and assimilation. While filtration has a temperature limitation, respiration increases exponentially with temperature (Fig. S1). Tissue growth functions are not affected by carbonate chemistry variables, as experimental studies have found that neither filtration (Lemasson et al., 2018) nor respiration (Beniash et al., 2010; Matoo et al., 2013) of oysters are affected by pH changes; however, net calcification is a function of Ω_{Ca} and temperature. Shell growth is a function of both total tissue weight and net calcification.

2.2 Present day reference simulation

A realistic reference simulation was generated to represent 2017 conditions. The year 2017 was chosen for atmospheric, terrestrial, and open-ocean boundary conditions as this represents a relatively typical hydrological year. Atmospheric forcings (air temperature, long- and short-wave radiation, precipitation, winds, dewpoint temperature, and air pressure) are obtained from the ERA5 atmospheric reanalysis (Copernicus Climate Change Service, 2017; Hersbach et al., 2020). Surface atmospheric variables are available at 3-hourly intervals with a 0.25° resolution and are interpolated to a 0.2° grid. Terrestrial inputs of freshwater, nitrogen, carbon, and sediment are

derived from the Phase 6 CBP Watershed Model (CBPWM; Bhatt et al., 2023) and USGS data. Daily estimates of freshwater discharge, water temperature, and loadings of nitrate, ammonium, organic nitrogen, and four classes of sediment from the CBPWM were concatenated to 74 locations throughout the model domain. To compute carbon loadings, constant carbon-to-nitrogen ratios are used, specifically 10:1 for dissolved organic matter (Hopkinson et al., 1998) and 6.625:1 for particulate organic matter (Redfield, 1934). Riverine TA concentrations are computed as in Da (2023), using monthly-varying linear relationships between historical USGS observations of discharge and USGS TA estimates determined using the Weighted Regression on Time, Discharge, and Season (WRTDS; Hirsch et al., 2010) approach. Riverine DIC is calculated from daily riverine TA and daily DIC:TA ratios, linearly interpolated from the monthly climatology of USGS WRTDS DIC:TA in each tributary. As in Da (2023), open boundary conditions are derived from a recent 600 m resolution whole-bay implementation of ROMS (St-Laurent and Friedrichs, 2024). Initial conditions for the six-month spin-up were derived from previous model results (Da, 2023).

Since spring-spawned oysters are typically deployed in late spring through summer on oyster farms, the reference run was started on July 1st and spanned one full year, ending June 30th of the following year. Oyster sizes were initialized based on shell height approximations of a typical spring-spawned oyster at deployment in July (i.e., a few months old). Starting dry tissue weight was assumed to be 0.001 g for all oysters, back-calculated from the approximate height of an oyster at the time of deployment. Starting shell weights and heights were calculated from allometric relationships to be 0.144 g and 11.6 mm, respectively.

2.3 Comparison of reference simulation to in situ observations

In situ water quality monitoring observations are available since 1984 throughout the Chesapeake Bay. Specifically, the Chesapeake Bay Program's Water Quality Monitoring Program (CBP WQMP) conducts cruises in the Bay and its tributaries. On average, stations are sampled once monthly, with the exception of June through August in the mainstem, when sampling occurs twice. In this study, measurements of water temperature, salinity, O_2, pH (NBS scale), TSS, and POC are used from 16 CBP stations throughout the model domain, with depths ranging from 5 to 16 m (Fig. 1a; CBP, 2024). For all variables except TSS and POC, measurements are taken *in situ* using a YSI or Hydrolab® sonde roughly every one to two meters of the water column. TSS and POC are obtained from bottle samples at the surface, bottom, and at deeper stations, two additional depths above and below the pycnocline. TSS is determined by filtering a known volume of water through a pre-weighted filter and then re-weighing the filter after filtration and drying. POC is determined through combustion of a filter using an elemental analyzer (Olsen, 2012).

Model skill was evaluated by comparing results from the reference simulation to the CBP WQMP observations described above. Hourly outputs from the four closest grid cells to each CBP station were spatially interpolated to obtain results at each respective station. Multiple variables in ECB at the bottom level of the model, including temperature, salinity, O_2, pH, TSS, and POC, were compared with observations from the same station and time, within the bottom 10% of the water column (Table 1). Model bias and root-mean squared difference (RMSD) were computed for all aforementioned variables. Seasonal skill was also evaluated by comparing the 2017 reference run to CBP decadal averages (Figs. 2, 3). Decadal means were used for these comparisons, as once-monthly or once-seasonally sampling dates in 2017 bias outputs toward

conditions on the time of the month when the measurements were taken in 2017, and the purpose of the comparison was to examine how the model reproduces average seasonal variability.

When compared to 2017 WQMP observations and seasonal decadal averages, model skill of ROMS-ECBO is reasonably high (Table 1, Figs. 2, 3), and similar to other model implementations of the Chesapeake Bay (Irby et al., 2016). Temperature and salinity are reproduced relatively well year-round (Fig. 2a,b) with annual biases of only 0.2°C and -1.5, respectively (Table 1). Bottom O_2 and pH are slightly overestimated, exhibiting the greatest model-data misfit in the spring and summer months in the tributary channels (Fig. 2c,d). pH is overestimated by 0.2 units, which is within the accuracy of the electrode measurements. Observed POC concentrations in the York and upper Rappahannock are higher than simulated in the model and exhibit very high spatial variability (Fig. 3a). Despite the high spatial variability of the TSS observations (Fig. 3b), mean TSS (45 ± 54 mg L^{-1}) is captured within 1.1 mg L^{-1} by the model.

Growth rates determined using the EcoOyster equations and environmental outputs from ROMS-ECB were compared with oyster data collected in the York River (Paynter et al., 2008; Liddel, 2008; Kingsley-Smith et al., 2009; Degremont et al., 2012; Callam et al., 2016). Specifically, the tunable parameter (p) that limits oyster filtration was adjusted to provide a best match between the modeled oyster growth rates and the published rates. Multiple *p*-values were tested, and a value of p=0.15 resulted in modeled oyster growth that best matched published growth rates. The resulting shell growth predicted by the model was found to be close to the *in situ* data (52.0 ± 1.1 mm y^{-1} and 51.3 ± 2.9 mm y^{-1} for the model and observation means and standard deviations, respectively).

2.4 Future simulations

In addition to the reference run, this study generated five future simulations (Table 2) to investigate the change in carbonate chemistry conditions and oyster growth resulting from three drivers of future change in the bay: atmospheric CO_2 (*AtmCO₂*), atmospheric warming (*Temp*), and nutrient loading (*TMDL*). Model forcings were modified for each simulation to represent mid-century conditions. A *Combined Future* simulation was run including forcings of all future stressors, in addition to three sensitivity simulations to isolate the impacts of each stressor on oyster growth. Atmospheric CO_2 concentration for the *AtmCO₂* and *Combined Future* simulations was set to 655 ppm, derived from the Coupled Model Intercomparison Project Phase 5 report RCP8.5 (business-as-usual) scenario projected for 50 years in the future relative to the reference run (Meinshausen et al., 2011). Future atmospheric temperature for the *Temp* and *Combined Future* simulations was obtained from the IPSL-CM5A-LR Earth System Model (Dufresne et al., 2013), statistically downscaled with the Multivariate Adaptive Constructed Analogs method (Abatzoglou and Brown, 2012). IPSL-CM5A-LR was selected as in Hinson et al. (2023), since it was deemed the most representative downscaled ESM of the 20 available. As in Hinson et al. (2023), the delta method was used to calculate the daily average change in atmospheric temperatures between present-day and future conditions. To calculate this change, two 30-year climatologies, centered on 2000 and 2050 respectively, were computed and daily averaged 50-year differences between the two climatologies (Fig. 4) were added to the atmospheric temperatures used in the reference run. Future watershed inputs for the *TMDL* and *Combined Future* simulations included a climatology of nitrate, ammonium, dissolved organic matter, and particulate organic matter concentrations, derived from a Phase 6 CBPWM 1991-2000 run using reduced nutrient concentrations assuming the TMDLs had been successfully achieved (Bhatt et al., 2023).

Freshwater discharge in this run was set to be identical to the reference run, to isolate the effects of lowered nutrient concentrations on water chemistry and oyster growth. Since future climate change is expected to impact terrestrial inputs much less than future management actions (Irby et al., 2018), the direct impact of climate change on the watershed is not considered in this analysis. A fifth simulation (*AtmCO_2 + Temp)* was run to compare the influences of local management actions to the combined drivers of climate change, which includes both future atmospheric CO_2 concentration and atmospheric temperature. Preliminary investigations revealed a minimal impact of sea level rise on Ω_{Ca} in the bay; therefore, it was not included in the simulated climate change variables.

To generate open boundary conditions for each future simulation, a full bay model (St-Laurent and Friedrichs, 2024) was run with the same atmospheric and river forcings as in this 120-meter model implementation. As in the reference run, all future simulations were spun up for six months (January 1 – June 30) before beginning on July 1, but represent 50 years in the future from the reference simulation (i.e., July 1, 2067). Initial conditions for all spin-ups are identical to the reference simulation. Analysis confirmed the effects of initial conditions are negligible by July 1. To examine results most relevant to oysters, model output was extracted at locations that support oyster production, defined as all grid cells in which tissue weight exceeded 1 g at the end of the reference run (i.e., one year of growth; Fig. S2). All results shown are from the bottom level of the model, representing conditions similar to bottom cage aquaculture methods that are common in Virginia. Spatial variation in model outputs across grid cells in the model domain is reported using standard deviation.

3. Results

3.1 Reference run results

In the present-day reference run, the environmental variables used as inputs to the oyster parameterizations exhibit substantial seasonal (Fig. 5a-f) and spatial (Figs. 6, S3) variability. As expected, bottom temperature is highest in summer, reaching an average of 29.3 °C in July when averaged across grid cells that support oyster growth (Fig. 5a). Temperature is higher in the shallower parts of the tributaries compared to the channels (Fig. S3a). Bottom salinity exhibits higher values in the fall and winter, reaching a maximum average of 17.7 in October, and drops in the spring and summer to reach a minimum average of 12.3 in June (Fig. 5b). Annual average bottom salinity ranges from 0 to 26 throughout the model domain (Fig. S3b), with the highest values in the southern areas in closest proximity to the open-ocean. The seasonal cycle for bottom POC is similar to that of temperature, peaking at 1.7 g C m^{-3} in June and dropping to 0.57 g C m^{-3} in January (Fig. 5c). Bottom POC also varies widely throughout the model domain (Fig. 6a), with relatively higher values in the Rappahannock compared to the York River, along the shoals of the tributaries, and along the western shoals of the mainstem Bay north of the Rappahannock. Ω_{Ca} exhibits an annual cycle similar to that of temperature and POC, reaching a maximum average of 3.2 units in August and a minimum average of 1.1 units in January. Annual mean bottom Ω_{Ca} also varies widely throughout the model domain (Fig. 6d). Generally, bottom Ω_{Ca} increases with salinity, with low to zero values in the tidal fresh portions of the upper tributaries and higher values along the western shoals of the mainstem Chesapeake Bay. The opposite temporal pattern is seen in bottom O_2, which peaks at 12.3 mg L^{-1} in February and drops to an average of 6.3 mg L^{-1} in August (Fig. 5e). O_2 concentrations are highest along the shoals and lowest in the deep channels (Fig. S3c). Bottom TSS concentrations exhibit tidal variability throughout the year and are highest

in the York River with much lower concentrations observed in the other portions of the model domain (Fig. S3d). Environmental conditions averaged annually across grid cells that support oyster growth are provided in Table 3, and conditions averaged annually across all grid cells in the model domain are provided in Table S5.

Tissue and shell weights increase modestly from July through April, and the highest rates of increase are seen in May and June near the end of the one-year reference run (Fig. 5g,h). At the end of the reference run, the spatial patterns of shell and tissue weight are nearly identical (Fig. 7), as tissue growth largely drives shell growth (Table S4). Both shell and tissue weights are highest along the shoals of the York and Rappahannock Rivers (Fig. 7a,d) and low in the deeper waters where TSS concentrations are high (Fig. S3d). A wider region of high shell and tissue weight appears in the Rappahannock, while the highest weights in the York are confined to a very narrow and shallow strip along the coastline. Shell and tissue weights are higher along the southwestern than the northeastern coastlines of the tributaries, where the shoals are wider in both tributaries (Fig. 1a). Oyster growth metrics averaged across grid cells that support oyster growth are provided in Table 4.

3.2 Results of *Combined Future* simulation

All environmental variables examined exhibit change from the reference run in the *Combined Future* simulation. When averaged over the entire model domain, a temperature increase of 1.5 °C is projected (Table S5). Temperature and salinity are projected to increase across the entire model domain (Fig. S3a,b). Bottom POC is projected to decrease by 0.07 g C m^{-3} (Table S5), with POC reductions predicted to be most pronounced in the mid- to upper tributaries (Fig. 6c). Mid-century bottom Ω_{Ca} is projected to be lower throughout most of the region, with an average reduction of 0.8 units over the whole model domain (Table S5). The spatial distribution

of future Ω_{Ca} is generally consistent with present-day Ω_{Ca} patterns, and the greatest decreases are projected to occur in regions with the highest present-day Ω_{ca} (Fig. 6 d,e,f). An average reduction in O_2 of 0.3 mg L^{-1} is predicted across the model domain (Table S5), which will be mostly spatially uniform (Fig. S3c). TSS is projected to be reduced by 0.2 mg L^{-1} with high spatial variability in the projected change (Fig. S3d)

Changes in environmental conditions do not occur uniformly throughout the year. Temporal changes in environmental conditions averaged across grid cells that support oyster growth are provided in Figure 5. Annually averaged increases in temperature and salinity are the same when averaged over only grid cells that support oyster growth as they are when averaged across the entire model domain (Tables 3, S5). The greatest temperature increases are projected to occur in the warmer months, with an average increase of 1.6 °C predicted for June through August and an average increase of 1.2 °C predicted for December through February. Bottom temperatures are projected to surpass the optimal temperature for oyster filtration (27 °C) primarily in July and August (Fig. 5a). Salinity increases are projected to be greatest at the beginning of the year, with an average increase of 0.44 between January and March and an average increase of 0.20 for the remainder of the year (Fig. 5b). Bottom POC at grid cells that support oyster growth is expected to decrease slightly less than the average for the entire region (Tables 3, S5), with the greatest reductions in the spring and summer and little to no change in the winter (Fig. 5c). For $\Omega_{Ca,}$ O_2, and TSS, projected reductions are slightly greater at oyster growth sites than for the entire domain. Ω_{Ca} is projected to decrease by 0.9 units, with the greatest reductions expected to occur the warmer months (Fig. 5d). O_2 is projected to decrease year-round, though with slightly greater reductions in the winter (Fig. 5e) and an annual average reduction of 0.4 mg O_2 L^{-1} (Table 3). TSS is projected to decrease annually by 0.3 mg L^{-1} (Table 3), mostly in the spring, due to lowered POC (Fig. 5f).

Modeled shell and tissue weights after one year of growth are projected to decline in all regions that exhibit present-day growth, with the most severe reductions (up to 100%) occurring along the York and Rappahannock River shoals (Figs. 7c,f, 8). One-year tissue weight will be reduced by 1.3 g, on average, representing a 60% reduction across grid cells that support oyster growth (Table 4). Shell weight, which is largely driven by changes in tissue weight, is projected to be reduced by 11.4 g on average after one year of growth, representing a 68% reduction in average shell weight in regions that support oyster growth (Table 4). The greatest reduction in shell and tissue growth rates will occur in the warmer months near the end of the one-year simulation (-0.1 g d^{-1} from May through June), whereas the smallest change will occur in the winter months (-0.02 g d^{-1} from December through February), as the least growth occurs during that time (Fig. 5g,h). Shell thickness will be reduced by 61% on average (0.11 g mm^{-1}; Table 4).

Declines in year one shell weight will vary throughout the model domain (Fig. 8), following relative changes in bottom POC and Ω_{Ca} (Fig. 9). The mainstem has the most moderate reduction in shell weight relative to reference shell weight, with an average reduction of 31%, indicated by the slope of the scatterplot. Shell weights in the Rappahannock and York face the steepest reductions relative to reference, with average reductions of 86% and 96%, respectively, and a large portion of York oysters facing complete depletion of oyster tissue and shell in these locations (Fig. 9; indicated by proximity to 1:1 line). Proportional shell weight reductions in the mainstem are projected to correlate with POC reductions (Fig. 9a). For Ω_{Ca} in the mainstem, a group of sites face the greatest proportional reductions when Ω_{Ca} reductions are the greatest. However, for sites with lower proportional shell loss, the opposite trend is observed (Fig 9d). In the Rappahannock, higher POC reductions coincide with slightly lower proportional shell loss (Fig. 9b). Sites with the largest reductions in POC primarily occur in the York (Fig. 9c; see dark

blue symbols on the 1:1 line), and the greatest proportional shell weight reductions coincide with the greatest POC and Ω_{Ca} reductions (Fig. 9c,f). Similar results are found for tissue weight (not shown).

3.3 Results of individual future sensitivity simulations

Four individual future sensitivity simulations were conducted to isolate the specific mechanisms (increased atmospheric CO_2, increased atmospheric temperature, and/or nutrient reductions) causing the projected changes described above in the *Combined Future* simulation. The *AtmCO₂* sensitivity simulation produces substantial reductions in average bottom Ω_{Ca} (Fig. 10a) and, as expected, is not projected to impact bottom temperature, salinity, POC, O_2, or TSS (Table 3; Fig. 10d). The projected reduction in Ω_{Ca} is 0.9 units when averaged over oyster growth sites (Table 3), 0.1 units greater in magnitude than the average reduction for the entire model domain (Table S5), as greater reductions are expected along the shoals of the Rappahannock and mainstem shoal than the York and upper section of the Rappahannock (Fig. 10a). In this *AtmCO₂* simulation, shell weight is predicted to be most steeply reduced in the Rappahannock, with less impact in the York and mainstem regions (Fig. 11a). At grid cells with oyster growth, *AtmCO₂* produces a shell weight reduction of 6.3 g in comparison to the reference simulation, but no change in tissue weight (Table 4).

The *Temp* sensitivity simulation produces changes in all environmental variables impacting oyster growth (Tables 3, S5). Changes in temperature, salinity, and TSS will be identical to those from the *Combined Future* simulation (Tables S5, 3). Predicted reductions in POC and O_2 will be identical when averaged over only grid cells that support oyster growth as they are when averaged across the entire model domain (Tables 3, S5). POC reductions are expected to cover the majority of the model domain, with larger reductions in the upper Rappahannock (Fig. 10e). Spatial trends

in Ω_{Ca} change are similar to *AtmCO₂*, with smaller reductions in the tributaries compared to the mainstem, but less widespread overall and a lower average reduction (Table S5; Fig. 10b). Similarly, the average reduction across grid cells with oyster growth, 0.5 units, is less than the reduction predicted for the *AtmCO₂* simulation (Table 3). O_2 at oyster grid cells will exhibit a similar but slightly lower average reduction compared to *Combined Future* (Table 3). Patterns of change in shell weight in the *Temp* sensitivity simulation resemble those in the *AtmCO₂* simulation (Fig. 11b), with a greater predicted mean reduction of 8.4 g, a 50% decrease at grid cells with oyster growth (Table 4). Unlike *AtmCO₂*, tissue weight will decrease in *Temp*, by an average of 1.2 g, a 46% reduction (Table 4).

The *TMDL* sensitivity simulation produces a much smaller average change in environmental conditions than the *AtmCO₂* or *Temp* simulations (Tables S5, 3; Fig. 10c). *TMDL* does not influence temperature, salinity, or O_2 (Tables S5, 3), but produces POC and TSS reductions close to the averages for *Temp* (Tables S5, 3). While POC change in the *Temp* simulation is concentrated in the deeper portions of the tributaries (Fig. 10e), the POC reductions in the *TMDL* simulation are concentrated along the shoals of the tributaries, with the greatest reductions in the upper Rappahannock (Fig. 10f). Future change in Ω_{Ca} in this simulation is less than for *AtmCO₂* or *Temp* is largely confined to the upper Rappahannock shoals and in shallow tidal creeks throughout the study region (Fig. 10c). Patterns of change in shell weight will resemble *AtmCO₂* and *Temp* in the tributaries, but no change is predicted along the mainstem shoal (Fig. 11c). The *TMDL* simulation produces reduced shell (3.7 g) and tissue (0.5 g) weights, with a smaller negative influence on shell and tissue weight than *Temp* (Table 4; Fig. 11c, d).

Environmental conditions in the *AtmCO₂ + Temp* simulation are nearly identical to those in the *Combined Future* simulation (Tables 3, S5), with the exception of $\Omega_{Ca,}$ which is slightly

higher due to the absence of *TMDL*'s influence. As tissue growth is unaffected by Ω_{Ca}, tissue weight in this simulation is identical to that of the *Temp* simulation. Average shell weight reduction in *AtmCO₂ + Temp* is 10.2 g, slightly greater than from *AtmCO₂* or *Temp* alone, due to the combined influences of lowered tissue growth and lower Ω_{Ca}.

4. Discussion

This study provides high-resolution projections for oyster growing conditions and corresponding oyster growth in the Chesapeake Bay, with a specific focus on two Virginia tributaries. A high-resolution hydrodynamic-biogeochemical model was coupled with an Eastern oyster bioenergetics model and forced with future projections for atmospheric CO_2, temperature, and nutrient management. An overall reduction in Ω_{Ca} and oyster growth are predicted by mid-century throughout the study region under the combined effects of all three future stressors. Specifically, the greatest reductions in oyster growth are projected to occur in the York and Rappahannock Rivers, where unfavorable conditions for calcification will expand in the future and where food availability will be strongly impacted by warming and nutrient reductions. Bottom conditions in the York and Rappahannock rivers, particularly in the upper portions, will likely be unsuitable for aquaculture at mid-century on average, indicating climate change preparedness is critical for the oyster aquaculture industry.

4.1 Future projections of Ω_{Ca}

The magnitude of future change in Ω_{Ca} varies with present-day Ω_{Ca} conditions. Regions with high present-day Ω_{Ca}, primarily the mainstem shoals, are projected to experience the greatest reductions because of their low partial pressure of CO_2 (pCO_2) relative to fresher waters. Low pCO_2 water has a greater capacity for CO_2 uptake from the atmosphere than high pCO_2 water,

which is causing the fresher tributaries to experience smaller reductions in Ω_{Ca}. Acidic freshwater input often causes pCO_2 in the upper tributaries to exceed atmospheric pCO_2, causing outgassing (Cai et al., 2017; Shen et al., 2019b; St-Laurent et al., 2020; Cai et al., 2021). Since higher Ω_{Ca} regions will experience greater reductions than lower Ω_{Ca} regions (Fig. 5), the overall spatial variability of Ω_{Ca} will be reduced by mid-century, and more areas will experience conditions that are unfavorable for oyster shell-building.

Although future atmospheric CO_2, warmer temperatures, and reduced nutrient loading will all contribute to Ω_{Ca} reductions, the modeling experiments conducted here highlight that increasing atmospheric CO_2 is the largest contributor to decreases in Ω_{Ca} throughout the study region. Increased atmospheric CO_2 will cause reductions in Ω_{Ca} across the model domain, while warming is projected to contribute more to Ω_{Ca} reductions in the mainstem than in the tributaries. Nutrient reductions are expected to mainly influence Ω_{Ca} in shallow and fresh coastal areas, with little influence in oyster growing regions. Given the importance of atmospheric CO_2 in shaping future Ω_{Ca} conditions in the lower bay, reductions in anthropogenic carbon emissions will be necessary to lessen the projected impacts on carbonate chemistry in the Chesapeake Bay and globally.

Comparing our results to other studies examining the effects of acidification reveals that the Chesapeake Bay will likely acidify faster than the US West Coast. Siedlecki et al. (2021) projected a decrease of 0.8-1.0 in Ω_{Ca} in the Northern California Current System between 2000 and 2100. Projections from the present work indicate a similar magnitude of reduction in the lower Chesapeake Bay over a shorter time period (50 years), suggesting a faster rate of acidification in the lower bay. Feely et al. (2009) also reported that projections for Ω_{Ca} reductions are slightly greater in the Atlantic than in the Pacific. The relative differences in rates of acidification should be considered, however, in the context of present-day Ω_{Ca}. The Pacific Ocean has a higher ratio of

DIC:TA than the Atlantic, so present-day Pacific Ω_{Ca} is lower (Feely et al., 2004; Dunne et al., 2012). Therefore, while the Chesapeake Bay is acidifying faster, coastal Pacific waters may become undersaturated with calcite and aragonite sooner than in Chesapeake Bay. US West Coast shellfish mortality events associated with acidification or other climate change stressors may place increased pressure on US Atlantic fisheries to provide shellfish to the nation, highlighting the importance of climate change preparedness and resilience in the Chesapeake Bay region.

While atmospheric CO_2 is primarily responsible for changes in Ω_{Ca}, temperature and nutrient reductions are also projected to worsen carbonate chemistry conditions. Warming will reduce Ω_{Ca} by increasing community respiration and therefore DIC production in bottom waters, an influence that studies examining acidification and warming co-stressors in laboratory settings may be underestimating. Multi-stressor studies should consider simulating the synergistic effects of acidification and warming on carbonate chemistry conditions in order to better predict organismal responses to climate change. Our results also reveal how nutrient reductions influence Ω_{Ca} in coastal areas. Eutrophication can suppress acidification by increasing primary production (Borges and Gypens 2010; Shen et al., 2019; Da et al., 2021), and when simulating a reduction in eutrophication via nutrient management in our modeling study, the countering effect occurred. While the reduction in Ω_{Ca} from nutrient management is minor compared to the projected impacts of acidification and warming, its small contribution may shift Ω_{Ca} conditions from favoring net calcification to favoring dissolution, demonstrating the importance of considering multiple drivers when predicting exposure to ecologically relevant conditions of coastal acidification.

4.2 Future projections of oyster growth

Acidification, warming, and nutrient reductions are projected to affect shell and tissue growth of oysters in different ways. Here, increased atmospheric CO_2 caused reductions in shell growth of Eastern oysters due to its negative effect on Ω_{Ca} and thus calcification rates, which is consistent with experimental studies (Waldbusser et al., 2011; Gobler and Talmage, 2014). Shell weight reductions from increased atmospheric CO_2 were driven by changes in calcification rate alone, as tissue weight in EcoOyster is unaffected by Ω_{Ca} (Fig. 11d; Rivest et al., 2023). Experimental studies have identified indirect physiological impacts of elevated CO_2 on juvenile/adult oyster metabolism, growth, and reproduction (Beniash et al., 2010; Dickinson et al., 2012), suggesting that increased atmospheric CO_2 can sometimes influence tissue growth. Further investigation is necessary in order to include the relationship between atmospheric CO_2 and oyster tissue growth in our bioenergetics model. Under future warming conditions, lower bottom Ω_{Ca} compounds shell weight reductions from lowered tissue weight. Calcification rates are higher at warmer temperatures (Waldbusser et al., 2011), which will offset the negative effects of lowered Ω_{Ca} due to warming as long as Ω_{Ca} is still high enough to support calcification. However, as dissolution rates are also higher at warmer temperatures, warming may exacerbate shell weight reductions under conditions of extreme low Ω_{Ca}. Our results also show that nutrient reductions will lead to reductions in shell weight, largely driven by a reduction in tissue weight resulting from lower food availability (POC), rather than lower Ω_{Ca}.

While nutrient reductions are projected to have little influence on Ω_{Ca} in this study, their negative influence on food availability may be detrimental to tissue growth in certain parts of the study region, particularly the York River. Our model projections suggest that nutrient reductions may in some cases produce conditions that do not support any oyster growth along the shoals of

the York (Fig. 10f), a result of reductions in food availability that are predicted to be more substantial in the tributaries than the mainstem region (Fig. 6c). Multiple studies have demonstrated that Eastern oysters and other calcifying organisms perform better under acidification when they have sufficient food availability, as they are better able to keep up with the energetic demands of environmental stress (Thomsen et al., 2012; Ramajo et al., 2016; Schwaner et al., 2023). Therefore, nutrient reductions will likely influence oyster growth under acidification stress by different magnitudes in each tributary. When comparing the effects of local management actions to reduce nutrient runoff to the effects of climate change (increased atmospheric CO_2 and warming), it is evident that, on average, climate change will have a much greater influence on oyster growth (Table 4). However, the strong localized impacts of nutrient reductions in the York highlight the importance of examining the spatial variability of future changes in oyster growth. It is important for managers to consider local conditions when assessing the effects of nutrient reductions on oyster production.

Increased water temperatures are projected to slow oyster growth in the future. Specifically, large reductions in tissue weight are underpinned by three primary mechanisms: limitations on filtration at high temperatures (Loosanoff, 1958), increased respiration rates (Dame, 1972), and reduced food availability. In EcoOyster, the optimal temperature for Eastern oyster filtration is 27°C (Cerco et al., 2005; Jordan, 1987), and under warming, the frequency at which ambient temperature will surpass this optimal temperature will be higher (Fig. 7a), therefore causing more frequent declines in filtration rate (Cerco et al., 2005; Fulford et al., 2007). There is no clear optimal temperature for oyster respiration, and therefore it is assumed to increase exponentially with temperature (Hochachka and Somero, 2002). Thus, as oyster filtration rates begin to decline at high temperatures, respiration rates will continue to rise and decrease the

potential for tissue accumulation (Fig. S1). Previous studies on juvenile Eastern oysters do not support a consensus on the relationship between warming and tissue growth. Some report that growth is inhibited at higher temperatures (31°C, Stevens and Gobler 2018; 30°C, Speights et al., 2017). In contrast, Talmage and Gobler (2011) found no significant influence of high temperature (28°C) alone on tissue growth. The optimal temperature for oyster filtration may also vary among oysters, based on observations of maximum filtration rates of adult Eastern oysters occurring between 28.1°C– 32°C (Loosanoff, 1958). Variation in experimental design may have contributed to the contrast in results summarized here, in addition to the influence of local adaptation (Burford et al., 2014). Due to a lack of consensus on temperature limits of Eastern oyster filtration, further research is needed to more robustly represent oyster filtration in bioenergetics models and improve predictions of impacts of warming on oysters and their ecosystem services in the region.

Warming will likely have a negative effect on food availability for oysters. Compared to the effects of nutrient reductions, warming will have a much more widespread influence on POC, causing reductions throughout the model domain (Fig. 10e,f). In the tributaries, reductions in food availability from warming will be largest, but relatively less extreme than those from nutrient reductions in the shallow parts of the tributaries where oysters are affected. Remineralization of organic carbon in marine systems is temperature-dependent (López-Urrutia et al., 2016), and as warming occurs, remineralization of detrital carbon to DIC in bottom waters will occur at higher rates. As much of the lower bay is nutrient-limited (Zhang et al., 2020), phytoplankton growth rates will not increase much from warming alone; therefore, increased remineralization will likely reduce the overall amount of food available to oysters. Despite a similar reduction in food availability being predicted for future warming and future nutrient reductions, the influence of warmer temperatures will amplify the negative effects of reduced food availability on growth. In

this study, the critical temperature at which respiration rates exceed assimilation rates is dependent on filtration. When food availability limits filtration, this critical temperature lowers, and the temperature threshold for tissue loss is lowered. Experimental studies have demonstrated how organic carbon may be influenced by both warming and acidification (Simone et al., 2021), but as these dynamics can differ based on nutrient availability, it is important to consider how climate change will influence food webs and nutrient dynamics.

The projected mid-century reductions in oyster growth obtained from this analysis are consistent with the results of other studies that examine oyster growth under projected climate change conditions. A study modeling oyster responses in Barataria Bay, LA, for example, predicts that under a warming and high flow scenario (though without the effects of future nutrient reductions or atmospheric CO_2), oysters will experience widespread mortality in fresher parts of the bay by the end of the century (Lavaud et al., 2021). Experimental studies have shown similar negative effects of acidification, warming, lower food availability, and increased freshwater flow on oyster survival (LaPeyre et al., 2013; Rybovich et al., 2016; Lowe et al., 2019; Jones et al., 2019). Da (2023) found that the reductions in salinity and Ω_{Ca} that result from high discharge events in the York River will increase in extent as climate change progresses and increasingly threaten aquaculture production. In the Chesapeake Bay, extreme precipitation events are predicted to occur more frequently with future climate change, however an overall decline in annual average precipitation is also predicted (St. Laurent et al., 2021). As a result, the overall impact of freshwater from the land is not projected to change significantly in the future (Hinson et al., 2023). Changes in precipitation were thus not simulated in this study, but future work could examine the dynamics of climate change, salinity, Ω_{Ca}, and oyster growth in a year with more heavy rainfall events but lower annual rainfall.

4.3 Influence of future changes in oyster growth on aquaculture

Understanding the relative impacts of global climate change and local nutrient management actions on oyster growth and survival will allow aquaculture producers to anticipate how their oyster stock may respond to these anthropogenic changes. As the effects of climate change are subject to natural interannual variability, the magnitude of acidification and warming in a given year will likely differ (Cai et al., 2021; Moore-Maley et al., 2016; Li et al., 2016), influencing oyster growth through differing mechanisms. Smaller oysters resulting from slower growing times in a particularly warm year may present a different challenge to growers than weak-shelled oysters in a year with lower Ω_{Ca} and average temperatures. Mortality may also become a more urgent challenge as summer temperatures warm. A previous study examining commercial performance of Pacific oysters in Brazil found that interannual variability in temperature, chl*a* abundance, and climate events influenced survival and growth phase timing (Mizuta et al., 2012). High temperatures inhibited survival of oyster seed in that study, which frequently occurs in Pacific oysters (*Crassostrea gigas)* during the summer months in Europe and California (Goulletquer et al., 1998; Burge et al., 2007; Malhan et al., 2009). A similar phenomenon has been observed in Eastern oysters; however, mortality events in this species have not been conclusively linked to warmer water temperatures (Guevelou et al., 2019; Biranik & Allam, 2023), and the cause is yet to be resolved for either species. Nonetheless, the increasing occurrence of spring/summer mortality in Eastern oysters suggests that shifting the time of planting of oysters on leases later in the year may help mitigate the risk of widespread mortality, although the economic tradeoffs involved in shifting the growing season for oysters should be taken into account.

Future climate change and nutrient management are projected to worsen conditions for oyster growth, and the spatial variation in these changes may unevenly influence aquaculture

production. While reductions in shell and tissue growth are predicted for nearly all regions where oysters grow, these changes will likely differ based on present-day environmental conditions. Under present day conditions, the most oyster growth is projected to occur in regions with some of the highest present-day Ω_{Ca} and the greatest projected Ω_{Ca} reductions, i.e., in the Rappahannock River and mainstem shoals. Some of the most dramatic tissue and shell reductions are projected to occur in the York and upper Rappahannock, where reduced food availability and low Ω_{Ca} will limit oyster filtration and shell growth. Oysters in parts of both the Rappahannock and York Rivers will likely face mortality (represented by near complete depletion of oyster shell and tissue) by mid-century (Figs. 8, 9). However, these reductions will not be spatially uniform, underscoring the importance of oyster farm site selection within a tributary. In contrast, oysters grown outside the tributaries are projected to exhibit a smaller decline in growth, indicating greater future opportunity for oyster farming in these locations. Under the business-as-usual climate change trajectory analyzed here, bottom conditions in the tributaries will be less suitable for oyster aquaculture by mid-century, and producers might consider alternate farm locations or shifting production methods toward floating culture to avoid exposure to low Ω_{Ca} conditions.

Beyond reduced oyster growth, aquaculture operations may also be affected in the future by temporal changes in optimal growing conditions. Due to the input of freshwater that lowers DIC and TA and increases pCO_2 (Cai et al., 2017; Cai et al., 2021; Da, 2023), the greatest magnitude of Ω_{Ca} reductions occurs in spring. The majority of oyster growth is projected to occur in the spring and summer (Fig. 7), so changes to growing conditions may be most consequential during these warmer months. Deployment of oyster seed generally begins in the spring and continues into the summer, so it is important for producers to be aware of ambient conditions being experienced by their newly deployed oysters. As spring temperatures warm, phytoplankton blooms

will likely occur earlier in the year, shifting the time when food availability is highest (Da et al., 2021). Oysters deployed earlier in the year may benefit from greater food availability and perform better than oysters deployed in July or August when waters are warmest. For oyster farms closer to freshwater sources, the combined effects of low Ω_{Ca}, low salinity, and high summer temperatures may severely inhibit growth and extend time-to-market.

4.4 Future work

Providing the aquaculture industry with the best existing estimates of climate change impacts to their operations will allow them to make more informed decisions about their future practices. This study used a 120-meter horizontal resolution model grid to examine near-lease-level effects of climate change and management actions on oyster growth in a section of the lower Chesapeake Bay. Similar studies with high resolution model grids in other systems will strengthen our understanding of how regional anthropogenic effects will influence the oyster aquaculture sector and could be used to identify areas of opportunity for new aquaculture practices (Swam et al., 2022; Palmer et al., 2021; Lavaud et al., 2024). The present study incorporated one Earth System Model and one emissions scenario; future work should quantify how these choices impact estimates of future Ω_{Ca} and oyster growth (e.g., Hinson et al., 2023). Future modeling studies should also incorporate other climate change impacts, such as sea level rise and increased storminess which are projected to influence conditions for oyster growth in the Chesapeake Bay region (Seneviratne et al., 2012; Lowe et al., 2019, Rybovich et al., 2016, Jones et al., 2019).

To improve estimates of shell and tissue growth of oysters under climate change, additional experimental studies should be conducted to reduce the data gaps that currently limit model formulations. Uncertainties in the functional relationships and rate parameters used in these models may lead to an inaccurate influence of some environmental variables on oyster growth. For

example, results in this study may be particularly sensitive to the optimum temperature of filtration rate. Reductions in tissue weight are particularly dramatic when average temperature conditions at oyster lease sites remain above this optimal temperature from mid-June through late August, a vital time for oyster growth. As a result, growth in the model is sensitive to the simulation start date, and future studies should compare the influence of warming on growth in simulations that start at different times in the year. Many physiological studies of temperature impacts on oyster filtration date back to the mid-to-late-20th century, and present-day seasonal extremes that coastal organisms experience may routinely exceed the maximum temperatures used in many of these earlier experimental designs. For example, Jones (1987) used a maximum temperature of 27 °C, which was the ambient temperature when samples were collected in July from the Choptank River, MD. Between 1985 and 2014, bottom waters of the north mesohaline Bay main stem (closest to the Choptank) warmed 1.01 ± 0.13 °C during May to October (Hinson et al., 2022), and the present study predicts a 1.5 ± 0.26 °C increase across the entire model domain between 2017 and mid-century. To build stronger models of future climate impacts, and to expand scientific understanding of physiological limits of the Eastern oyster, future studies should re-examine temperature limitations on oyster filtration by using higher experimental temperatures.

As oyster growth is highly sensitive to food availability, improved measurements of particulate organic carbon in the region would fortify projections of oyster production under future climate change and nutrient management. Here, it is assumed that oysters feed on POC, a combination of plankton and detritus. However, average POC concentrations are highly spatiotemporally variable in the Chesapeake Bay due to eutrophication and algal blooms. In this study, POC was underestimated in the tributary channels; however, it is unclear how well POC was estimated in oyster growing areas, as *in situ* measurements are currently limited to stations in

the channels during monthly or semi-monthly sampling cruises. More routine POC measurements, as well as measurements of POC in regions where oyster farming operations occur, are needed to verify the spatiotemporal dynamics of food availability. Improved measurements of oyster food availability would allow for stronger model skill assessment and improved projections of oyster production.

5. Conclusions

This study predicts widespread reductions in Ω_{Ca} in the lower Virginia tributaries of the Chesapeake Bay by mid-century, highlighting the use of high-resolution model projections to better understand present-day carbonate chemistry conditions and to predict the effects of climate change on a region of high interest for aquaculture production. While similar modeling studies have projected acidification conditions in coastal regions with 3D coupled models (Siedlecki et al., 2021a,b; Fujii et al., 2021) or modeled oyster growth with remote-sensing data and dynamic energy budget models (Palmer et al., 2020; Palmer et al., 2021; Bertollini et al., 2021), the present study projects both carbonate chemistry conditions and oyster bioenergetics in the Chesapeake Bay with the highest resolution thus far. Specifically, widespread reductions in Ω_{Ca} will negatively impact oyster growth, with implications for aquaculture operations and local and regional economies. As bottom conditions worsen, site-selection for oyster farms or other adaptive measures will become imperative to sustain production and reduce the impacts of low Ω_{Ca} on farmed oysters.

Increased atmospheric CO_2 and warming are projected to inhibit oyster calcification, and warming and nutrient reductions will reduce oyster tissue and shell growth due to limitations on filtration and lowered food availability. While the effects of global climate change on oyster

growth are projected to be much stronger overall than the effects of local nutrient management, lowered food availability from nutrient reductions may have a strong influence on oyster growth in certain parts of the study region. As a result, all areas will not be equally vulnerable to future changes in the atmosphere and watershed. Understanding how individual drivers influence oyster growth is important for predicting effects on aquaculture production in the context of interannual variability of climate change and nutrient management outcomes. While the negative effects of temperature on growth were strong in this study, additional studies on Eastern oyster temperature limits are needed to improve projections, particularly as summer mortality of oysters is already common. Increased *in situ* measurements of biogeochemical variables and experimental studies on oyster physiology and bioenergetics will allow for improved projections of mid-century conditions and their potential impacts on oyster growth and the aquaculture industry.

TABLES

Table 1. Model skill statistics (mean ± standard deviation) comparing bottom grid cells from the reference run to Chesapeake Bay Program observations from the same station location and time, within the bottom 10% of the water column.

Variable	Model	Observation	Model Bias	RMSD[a]
Temperature (°C) n = 130	17.0 ± 9	16.7 ± 9	+ 0.2	0.7
Salinity n = 127	13.9 ± 7	15.4 ± 7	-1.5	2.7
Oxygen (mg O_2 L^{-1}) n = 130	8.0 ± 2.3	7.2 ± 2.9	+0.9	1.3
pH n = 74	7.8 ± 0.4	7.6 ± 0.4	+ 0.2	0.4
TSS (mg L^{-1}) n = 74	44 ± 34	45 ± 54	-1.1	48.3
POC (g C m^{-3}) n = 74	0.7 ± 0.3	1.7 ± 2.1	-1.0	2.4

[a]RMSD = root mean squared difference

Table 2. Experimental design for future simulations conducted for comparison to reference run. Model forcings include a combination of 2017 (reference) and 2067 (future) inputs of atmospheric CO_2, atmospheric temperature, and terrestrial nutrient loadings.

Future Simulation Name	Atmospheric CO_2	Atmospheric Temperature	Terrestrial inputs
Combined Future	Future	Future	TMDL[a]
AtmCO_2	Future	Reference	Reference
Temp	Reference	Future	Reference
TMDL	Reference	Reference	TMDL
AtmCO_2 + Temp	Future	Future	Reference

[a]TMDL (Total Maximum Daily Load) forcing includes inputs of nitrate, ammonium, and dissolved and particulate organic matter under the assumption that the nutrient reduction goals (EPA, 2010) are met.

Table 3. Bottom environmental variables for each model simulation (annual mean ± standard deviation) for grid cells that support oyster growth in the reference run (defined as those with greater than 1g dry tissue weight after one year of growth; Fig. S2). Analogous results averaged over all model grid cells are shown in Table S5.

Model Simulation	**Temperature (°C)**	**Salinity**	**POC (g C m^{-3})**	**Ω_{Ca}**	**Dissolved Oxygen (mg O_2 L^{-1})**	**TSS (mg L^{-1})**
Reference	17.0 ± 0.7	15.7 ± 2.1	1.12 ± 0.1	2.5 ± 0.49	9.1 ± 0.6	11.4 ± 5.8
Combined Future	18.5 ± 0.8	16.0 ± 2.1	1.03 ± 0.1	1.6 ± 0.35	8.7 ± 0.6	11.1 ± 5.9
AtmCO_2	17.0 ± 0.7	15.7 ± 2.1	1.12 ± 0.1	1.6 ± 0.35	9.1 ± 0.6	11.4 ± 5.8
Temp	18.5 ± 0.8	16.0 ± 2.1	1.07 ± 0.1	2.0 ± 0.32	8.8 ± 0.6	11.1 ± 5.9
TMDL	17.0 ± 0.7	15.7 ± 2.1	1.08 ± 0.1	2.4 ± 0.53	9.1 ± 0.6	11.2 ± 5.9
Temp + CO_2	18.5 ± 0.8	16.0 ± 2.1	1.07 ± 0.1	1.7 ± 0.33	8.8 ± 0.6	11.1 ± 5.9

Table 4. Modeled oyster characteristics from the end of each simulation (mean ± standard deviation) over grid cells that support oyster growth in the reference run (defined as those with greater than 1g dry tissue weight after one year of growth; Fig. S2).

Model Simulation	Shell Weight (g)	Tissue Weight (g)	Shell Thickness (g mm^{-1})
Reference	16.8 ± 10.9	2.2 ± 1.5	0.18 ± 0.08
Combined Future	5.4 ± 5.7	0.9 ± 0.8	0.07 ± 0.05
AtmCO_2	10.5 ± 8.0	2.2 ± 1.5	0.12 ± 0.06
Temp	8.4 ± 8.6	1.2 ± 1.1	0.10 ± 0.07
TMDL	13.1 ± 8.2	1.7 ± 1.2	0.15 ± 0.06
Temp + CO_2	6.6 ± 7.1	1.2 ± 1.1	0.08 ± 0.06

FIGURES

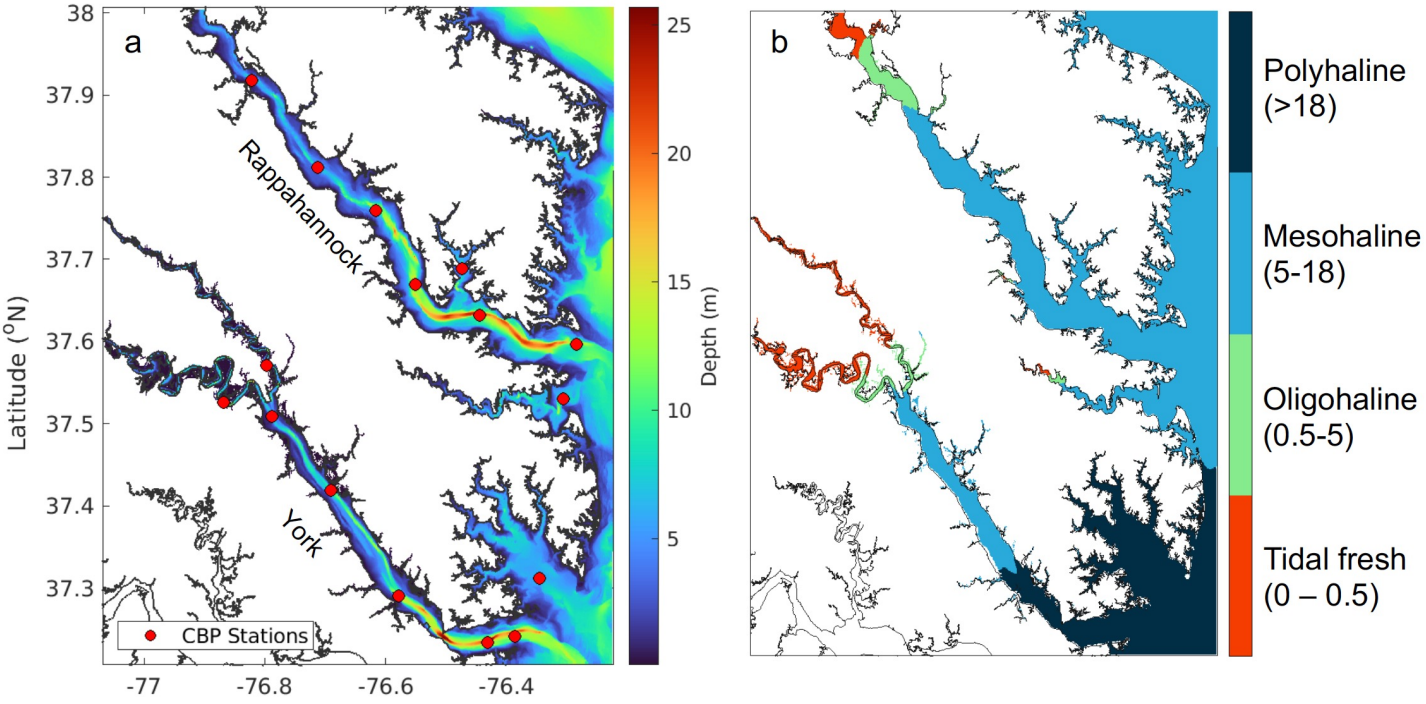

Figure 1. ROMS-ECBO model domain of Chesapeake Bay tributaries illustrating (a) bathymetry in meters and locations of Chesapeake Bay Program water quality monitoring stations (red circles) and (b) bottom salinity zones.

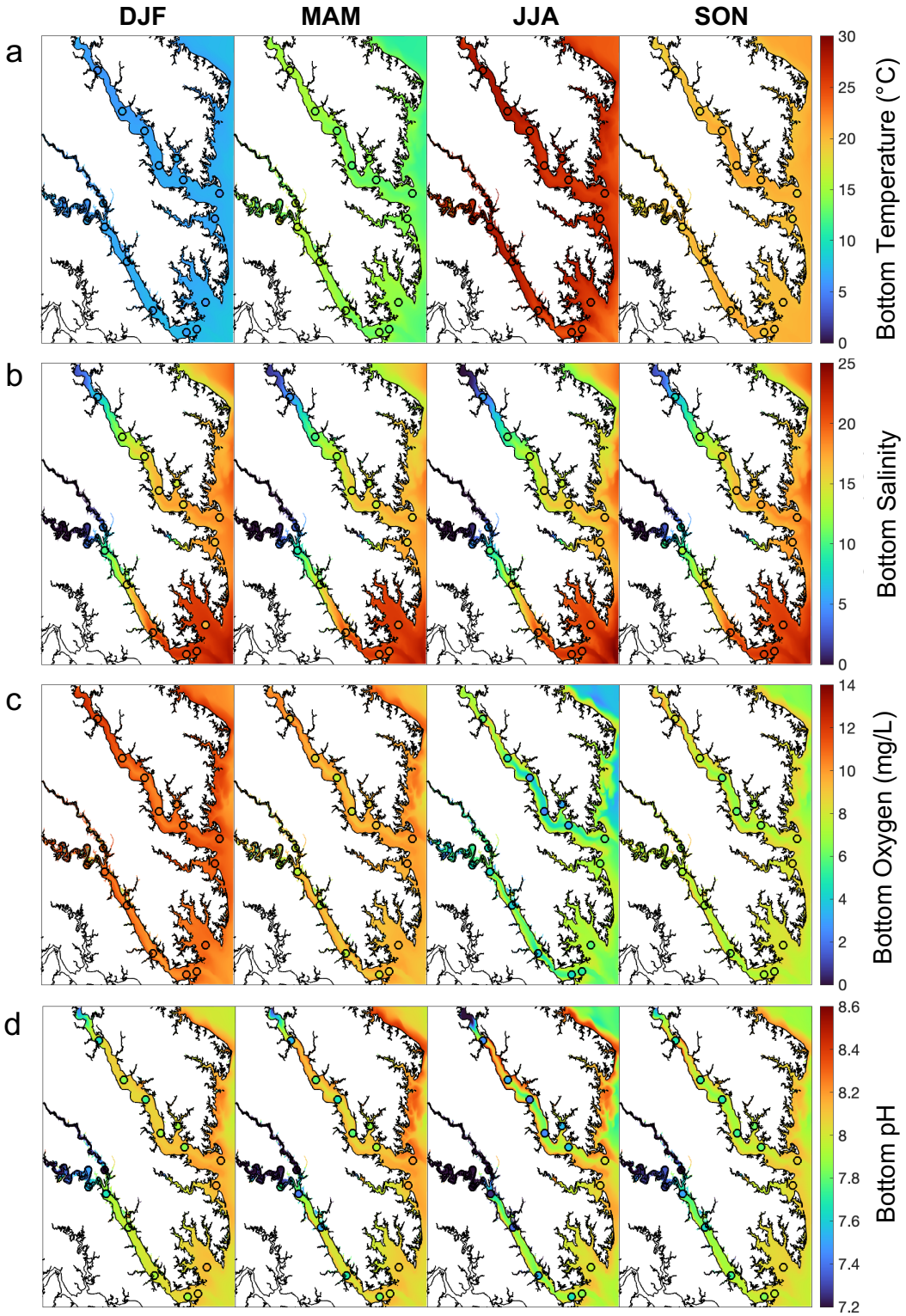

Figure 2. Seasonally-averaged bottom (a) temperature, (b) salinity, (c) dissolved oxygen, and (d) pH from the reference run. Circles represent seasonal decadal-averaged *in situ* observations at Chesapeake Bay Program stations (2010-2020). (DJF = winter, MAM = spring, JJA = summer, and SON = fall).

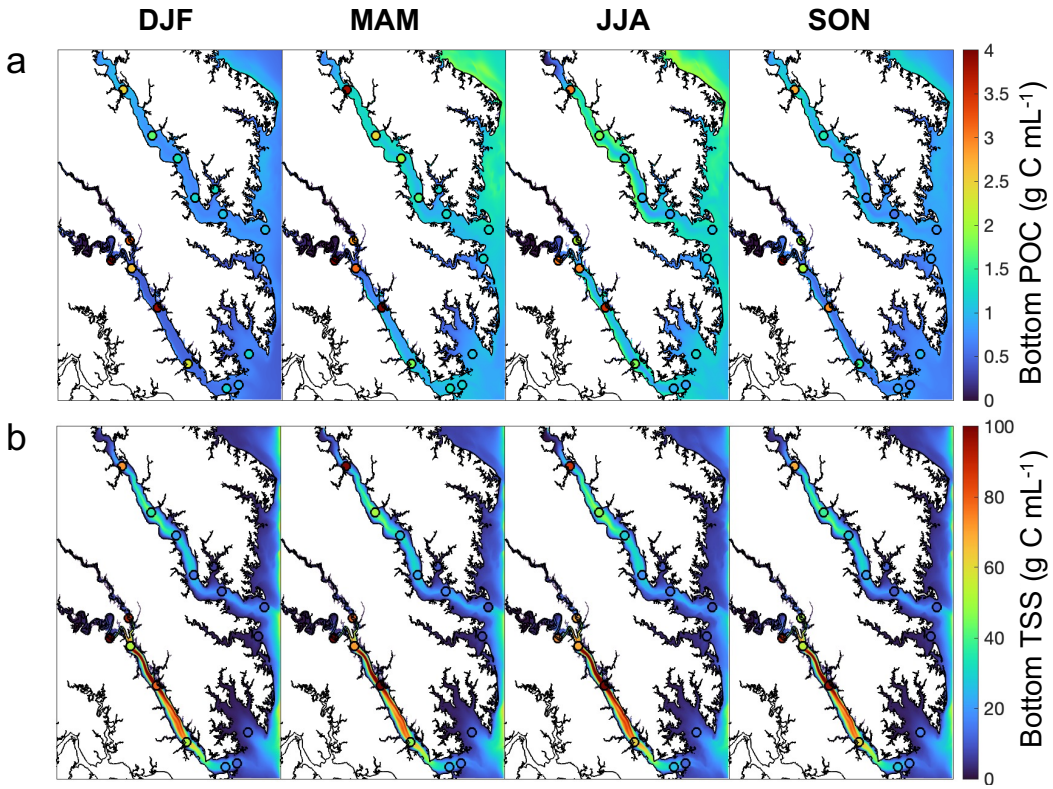

Figure 3. Seasonally-averaged bottom (a) POC and (b) TSS from output of the reference run of the ROMS-ECBO model. Circles represent seasonal decadal-averaged bottom measurements at Chesapeake Bay Program stations (2010-2020). (DJF = winter, MAM = spring, JJA = summer, and SON = fall).

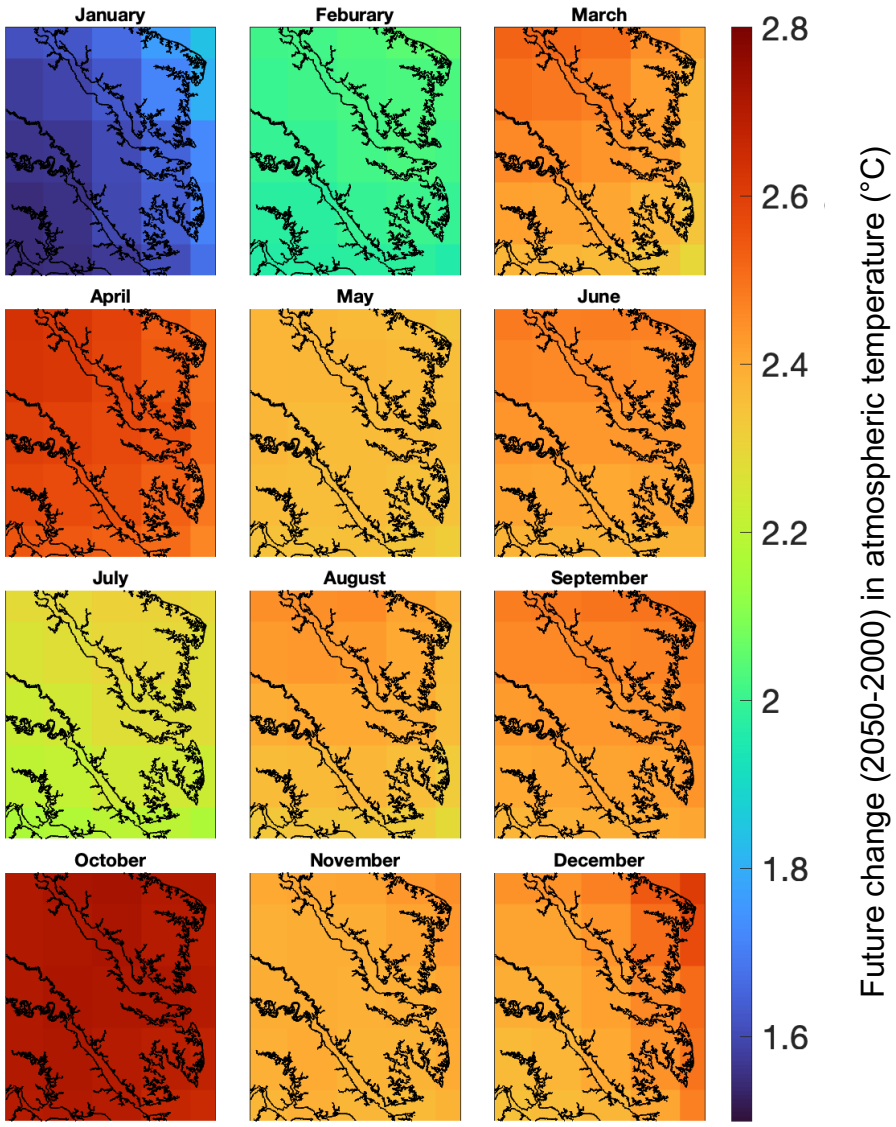

Figure 4. Monthly-averaged 50-year atmospheric temperature differences over the ROMS-ECBO model domain calculated as projections from 2050 minus those from 2000.

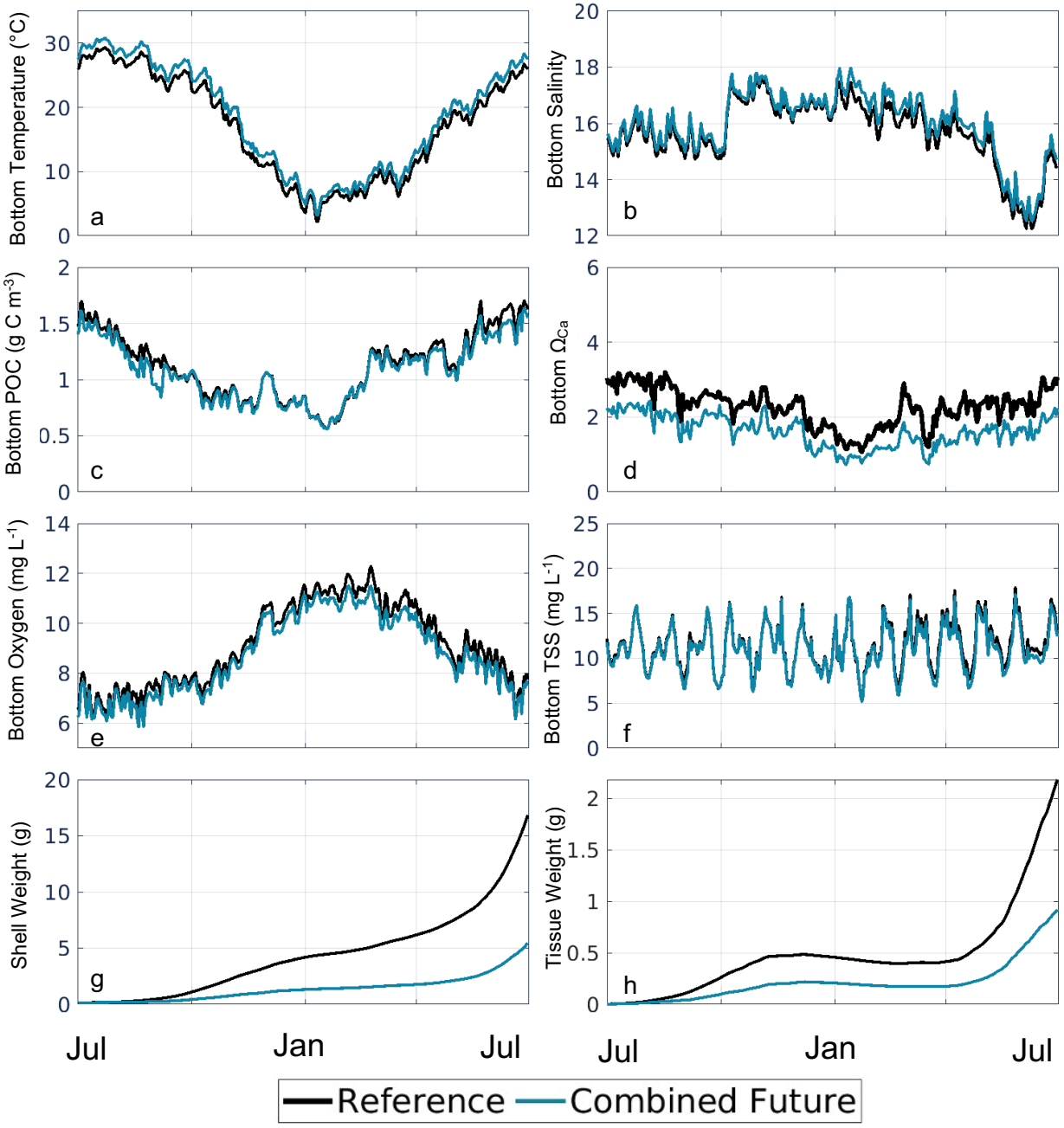

Figure 5. Time series of daily bottom (a) temperature, (b) salinity, (c) Ω_{Ca}, (d) POC, (e) shell weight, and (f) tissue weight, averaged over grid cells that support oyster growth in the reference run, for the present-day reference run (solid black line) and *Combined Future* simulation (dashed blue line).

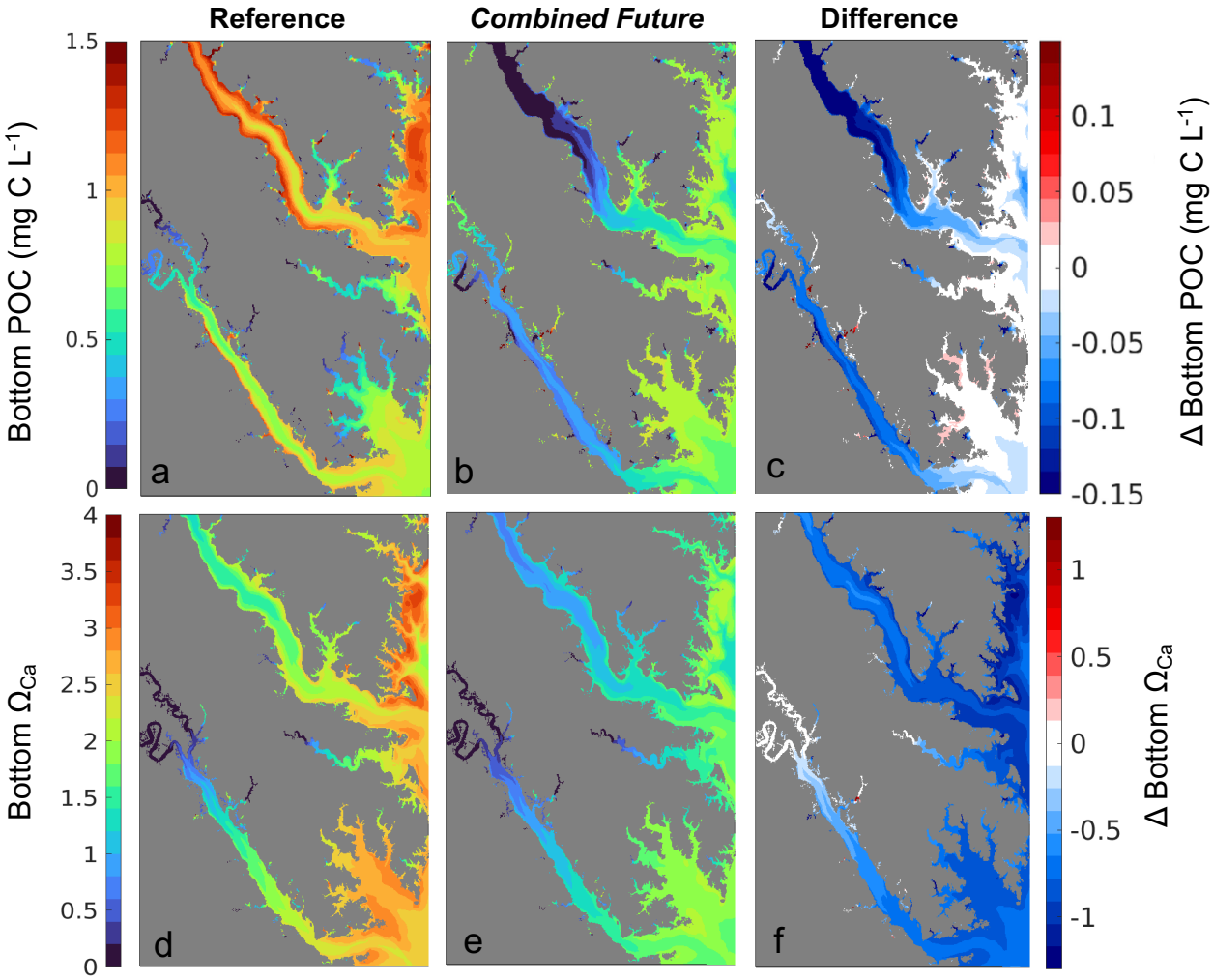

Figure 6. Annual mean bottom (a-c) Ω_{Ca} and (d-f) POC from (a,d) the present-day reference run, (b,e) the *Combined Future* simulation, and (c,f) the difference between (a) and (b), i.e., *Combined Future* minus reference.

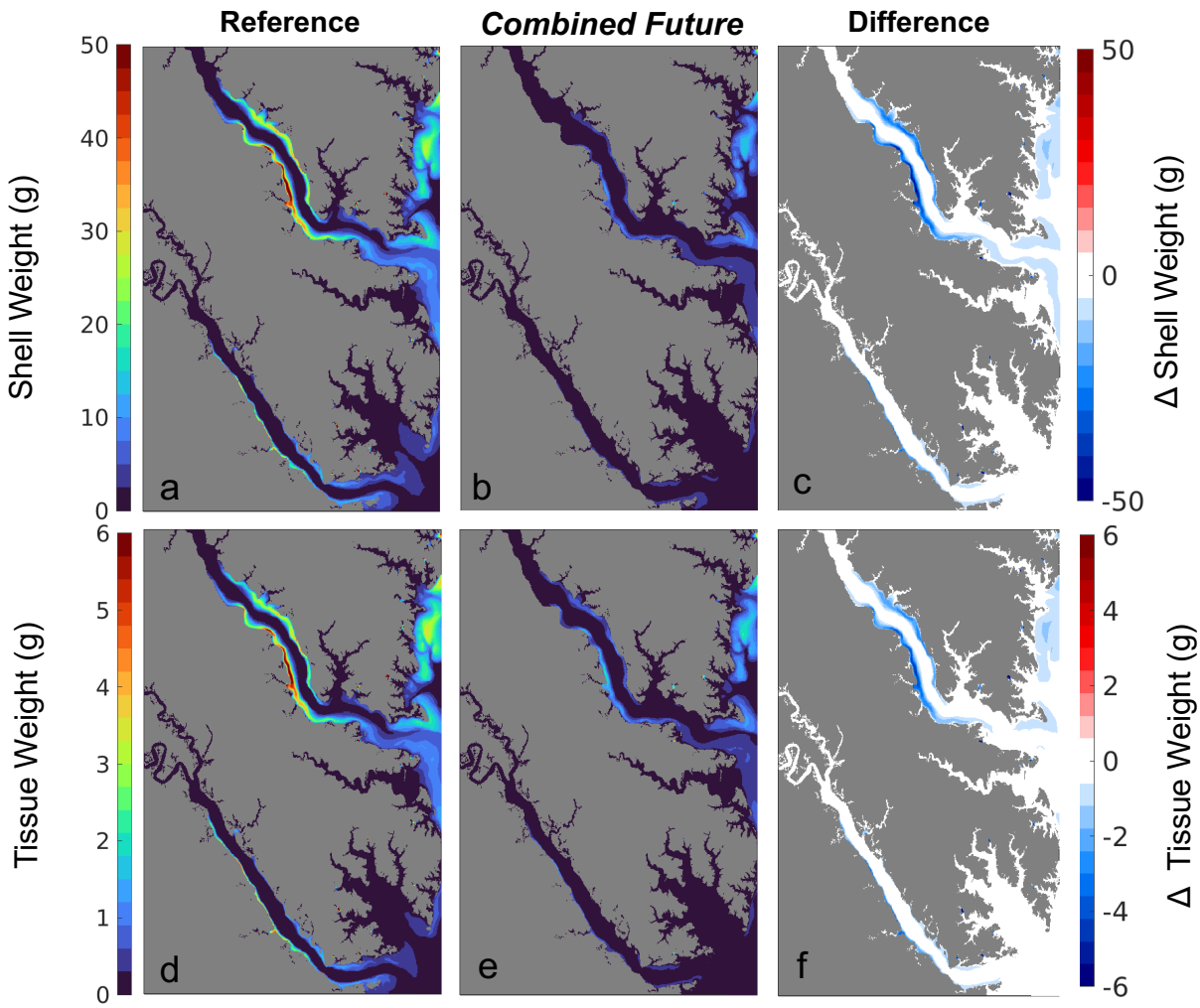

Figure 7. (a-c) Shell weight and (d-f) tissue weight at the end of the one-year simulation from (a,d) the present-day reference run, (b,e) the *Combined Future* run, and (c,f) their difference, i.e.,7777 *Combined Future* minus reference.

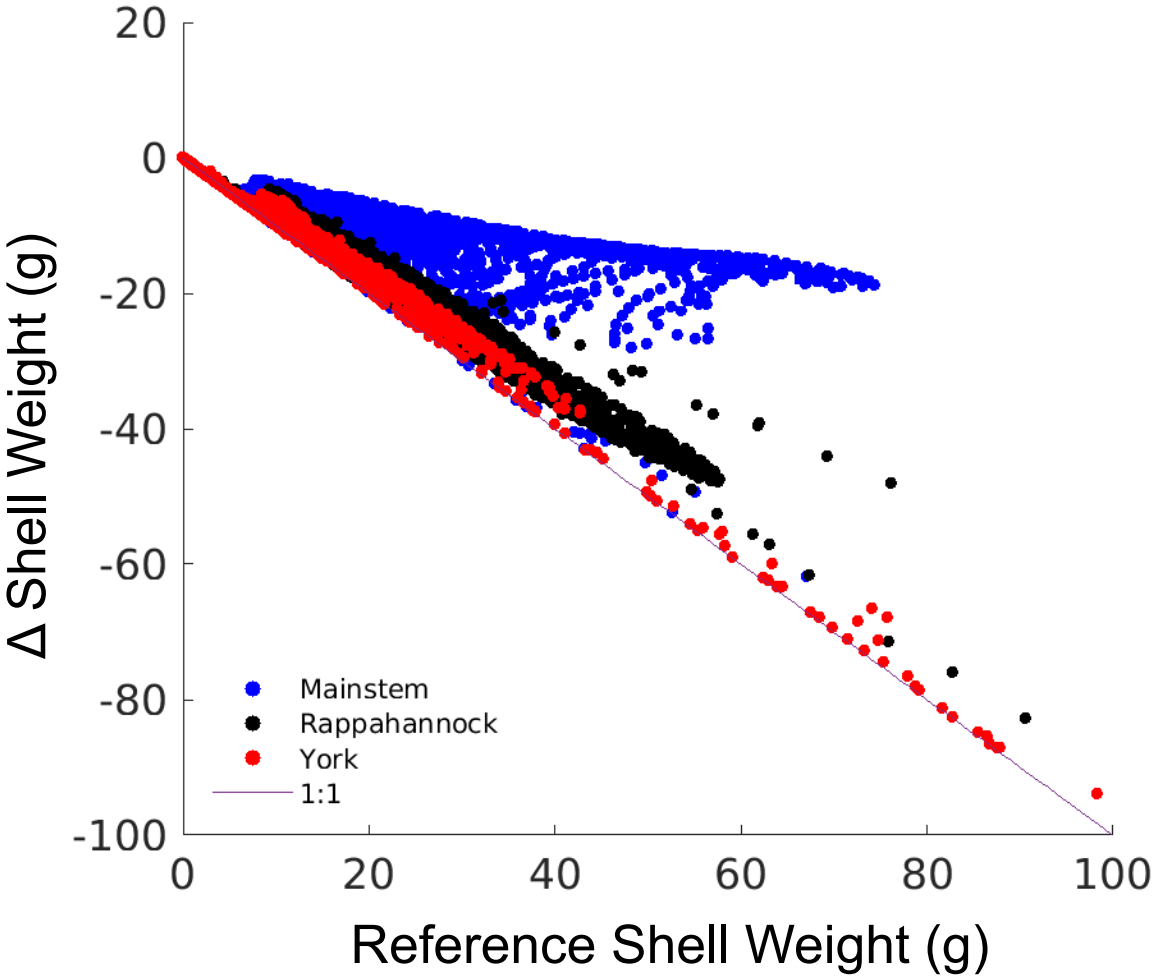

Figure 8. Difference in shell weight at the end of the one-year simulation between the *Combined Future* run and the reference run, i.e., *Combined Future* minus reference, colored by by region.

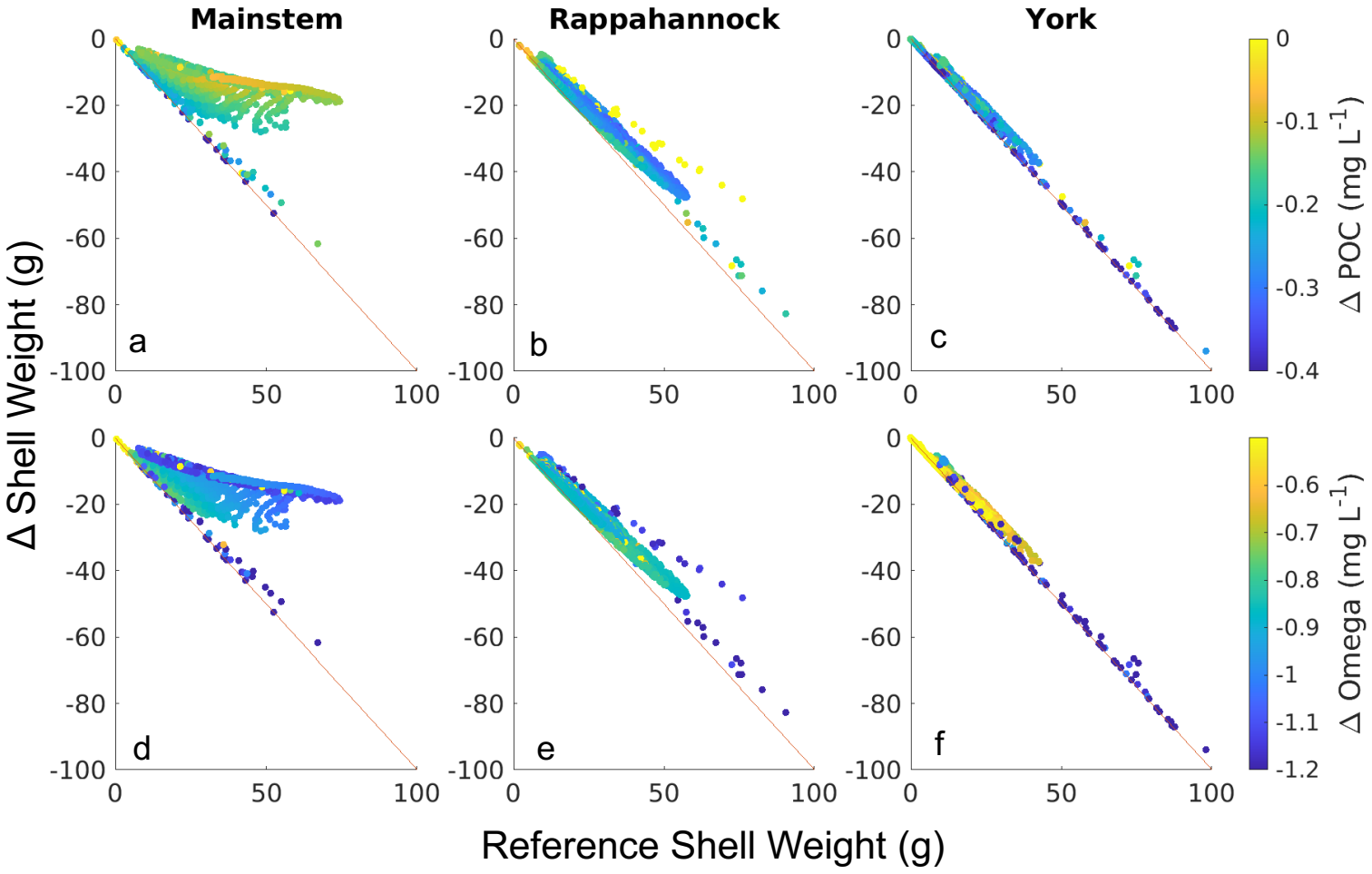

Figure 9. Difference in shell weight at the end of the one-year simulation between the *Combined Future* run and the reference run colored by (a-c) change in POC and (d-f) change in bottom Ω_{Ca} (i.e. *Combined Future* minus reference) for grid cells that support oyster growth. Results are presented for (a,d) the mainstem shoal only, (b,e) the Rappahannock River only, and (c,f) the York River only.

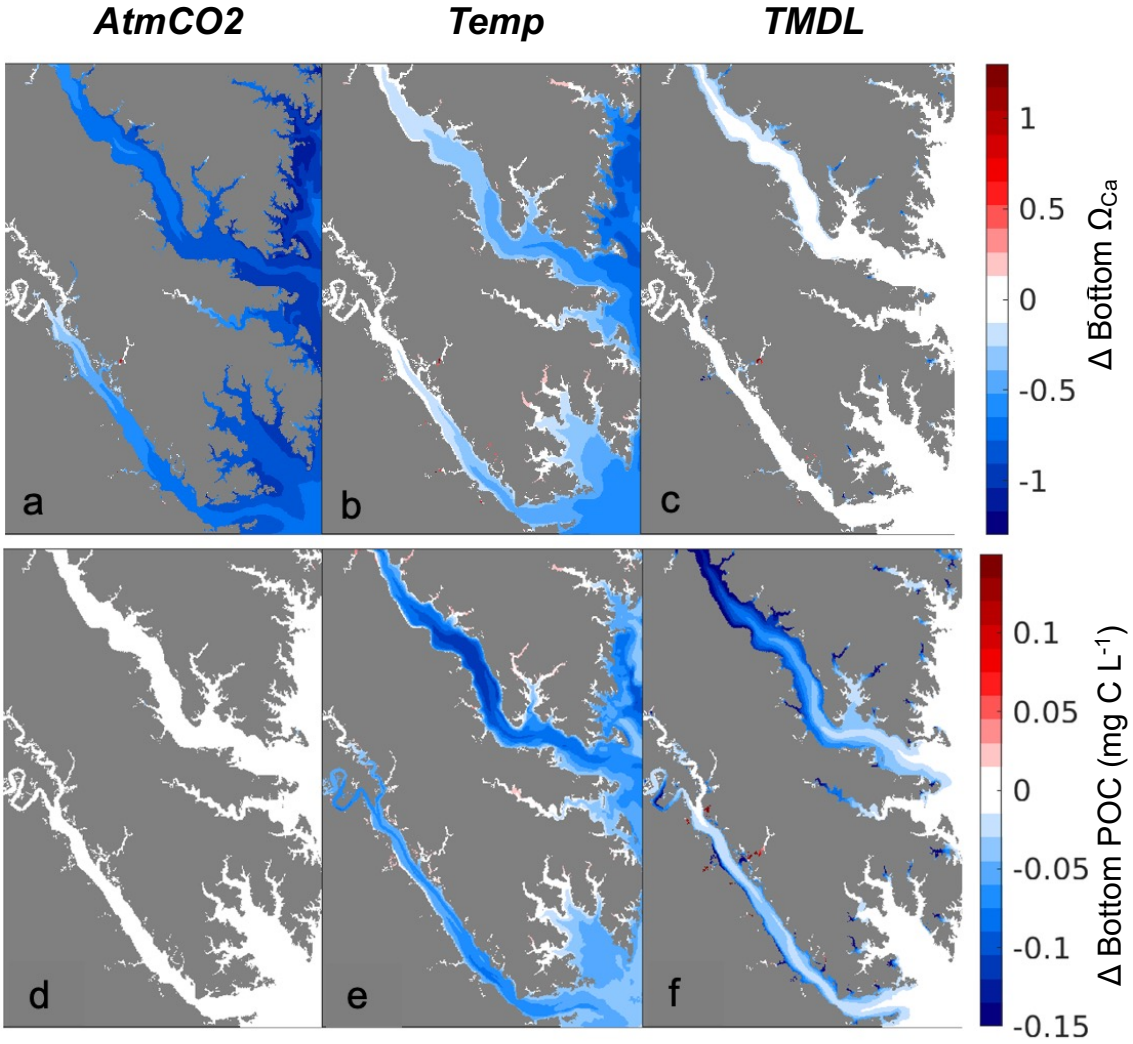

Figure 10. Differences in annual averaged (a-c) bottom Ω_{Ca} and (d-f) bottom POC (d-f) for three sensitivity experiments: (a) $AtmCO_2$, (b) Temp, and (c) TMDL. Differences represent future results minus those from the present-day reference run.

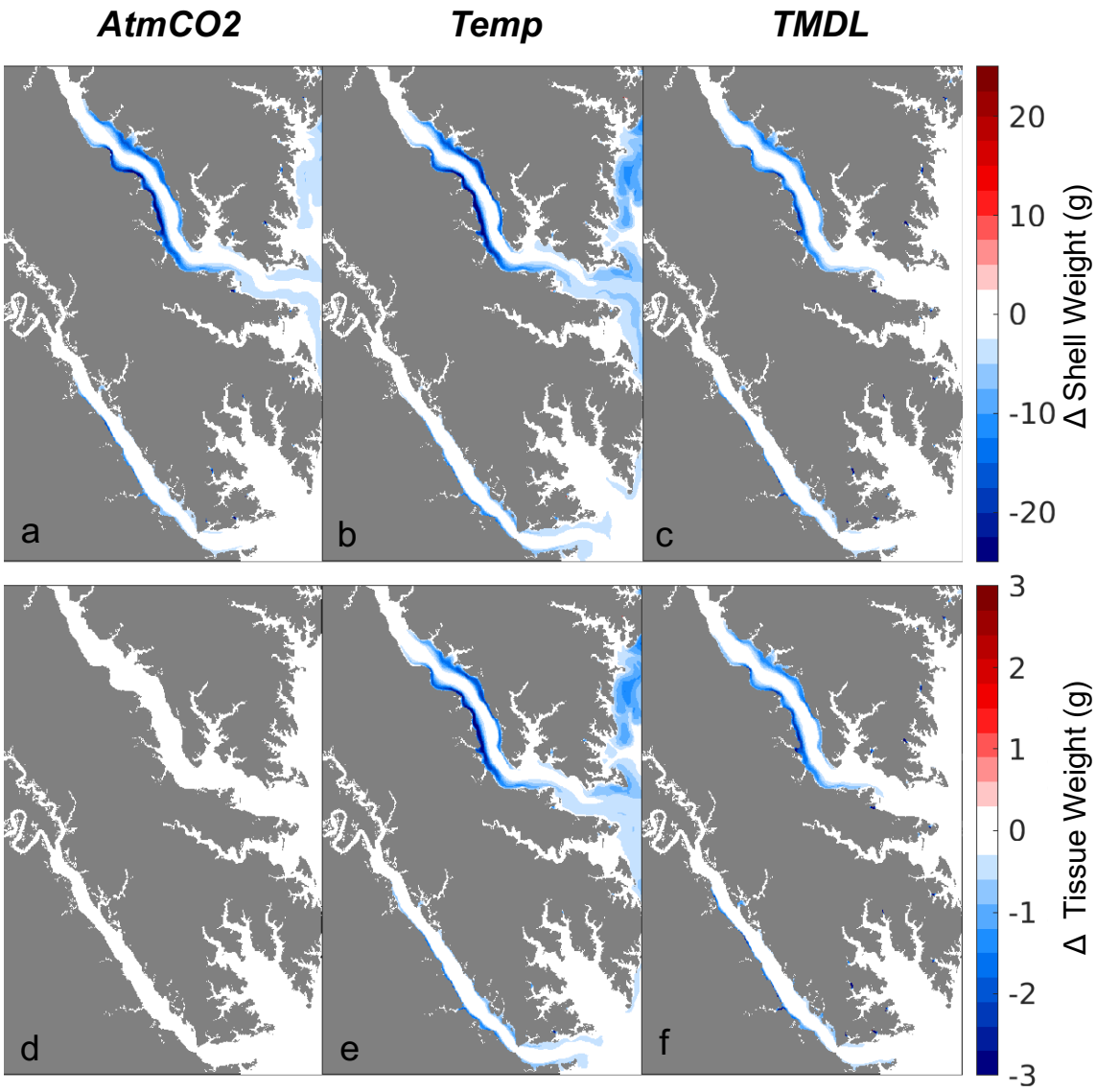

Figure 11. Differences in (a-c) shell weight and (d-f) tissue weight at the end of the one-year simulation for three sensitivity experiments: (a) AtmCO_2, (b) Temp, and (c) TMDL. Differences represent future results minus those from the present-day reference run.

SUPPLEMENTARY MATERIALS

Table S1: Growth functions in EcoOyster

Equation #	
1*	$w_j^{total} = w_j^{tissue} + w_j^{gonad}$
2*	$\frac{d}{dt} w_j^{gonad}(t) = reprod_j(t) - resorb_j(t) - spawn_j(t)$
3*	$\frac{d}{dt} w_j^{tissue}(t) = A_j(t) - R_j(t) - reprod_j(t) + resorb_j(t)$
4*	$\frac{d}{dt} w_j^{shell}(t) = net\_calcification(t)\, w_j^{total}$

*Sub-equations are provided in Table S2

Table S2: Supporting Equations for growth functions

Equation #	
5	$reprod_j(t) = \begin{cases} \max\left[0, A_j(t) - R_j(t)\right] rep_{eff}(t) & \text{for } j = 1, \\ 0 & \text{for } j = 2 \end{cases}$
6	$rep_{eff}(t) = \begin{cases} \min[\max(0, 0.054T(t) - 0.729), 1] & \text{for January to June,} \\ \min[\max(0, 0.047T(t) - 0.809), 1] & \text{for July to December} \end{cases}$
7	$resorb_j(t) = \begin{cases} \max[0, -(A_j(t) - R_j(t))] \dfrac{w_j^{gonad}}{w_j^{gonad} + K_{gonad}} & \text{for } j = 1, \\ 0 & \text{for } j = 2 \end{cases}$
8	$spawn_j(t) = \begin{cases} \max[0, \dfrac{w_j^{gonad}(t)}{w_j^{gonad}} - 0.2]\, w_j^{gonad} & \text{for } j = 1, \\ 0 & \text{for } j = 2 \end{cases}$
9	$A_j(t) = \frac{F_j(t) POC(t)}{C{:}dw} AE$ *C:dw = 0.45. AE = 0.75*
10	$R_j(t) = 0.0095\ (w_j^{total}(t))^{3/4} \exp[0.069(T(t) - 20°\text{C})] + A_j(t) RF$ *RF = 0.1*
11*	$F_j(t) = F_j^{max}(t)\, f_T(t)\, f_S(t)\, f_{tss}(t)\, f_{O2}(t)\, f_{chla}(t) p$ *p = 0.15*
12	$F_j^{max}(t) = 0.17\ (w_j^{total}(t))^{3/4}$
13	$net\_calcification(t) = a \dfrac{1 - \exp(-b(\Omega_{ca}(t) - c))}{1000} \exp[0.0271(T(t) - 25°\text{C})]$, *a* = 158.2, *b* = 1.052, *c* = 0.9323

*Environmental limitation functions are provided in Table S3

** j = 1 for diploids, j = 2 for diploids

Table S3: Dimensionless environmental limitation functions for filtration (Eq. 11, Table S2)

Equation #	
14	$f_T(t) = \exp\left[-0.006(T(\mathrm{t}) - 27°\mathrm{C})^2\right]$
15	$f_S(t) = \begin{cases} 0 & if\ S \leq 5, \\ 0.0926\,S(t) - 0.139 & if\ 5 < S < 12, \\ 1 & if\ S \geq 12 \end{cases}$
16	$f_{tss}(t) = \begin{cases} 1 & if\ TSS < 25, \\ 10.364\ (\ln TSS(\mathrm{t}))^{-2.04777} & if\ TSS \geq 25 \end{cases}$
17	$f_{O2}(t) = \left[\,1 + \exp\left(1.1\,\frac{1.75 - O2(t)}{1.75 - 1.5}\right)\right]^{-1}$
18	$f_{chla}(t) = \max\left[0,1 - \exp\left(-0.26(chla(\mathrm{t}) - 2.2)\right)\right]$

Table S4: Allometric equations for shell height and tissue and shell weight

Equation #	
19	$h^{shell\ allo} = 73.85(w^{total})^{0.2680}$
20	$w^{shell\ allo} = 58.05(w^{total})^{0.8681}$

Table S5. Bottom environmental variables for each model simulation (annual mean ± standard deviation) for all model grid cells.

Model Simulation	Temperature (°C)	Salinity	POC (g C m^{-3})	Ω_{Ca}	Dissolved Oxygen (mg O_2 L^{-1})	TSS (mg L^{-1})
Reference	16.9 ± 1.0	15.7 ± 5.8	0.81 ± 0.3	2.2 ± 0.75	8.6 ± 0.9	15.9 ± 18
Combined Future	18.4 ± 1.1	16.0 ± 5.8	0.74 ± 0.3	1.4 ± 0.53	8.3 ± 0.8	15.7 ± 18
AtmCO_2	16.9 ± 1.0	15.7 ± 5.8	0.81 ± 0.3	1.4 ± 0.52	8.6 ± 0.9	15.9 ± 18
Temp	18.4 ± 1.1	16.0 ± 5.8	0.76 ± 0.3	1.8 ± 0.61	8.3 ± 0.9	15.7 ± 18
TMDL	16.9 ± 1.0	15.7 ± 5.8	0.78 ± 0.3	2.1 ± 0.76	8.6 ± 0.9	15.8 ± 18
Temp + CO_2	18.4 ± 1.1	16.0 ± 5.8	0.76 ± 0.3	1.5 ± 0.52	8.3 ± 0.9	15.7 ± 18

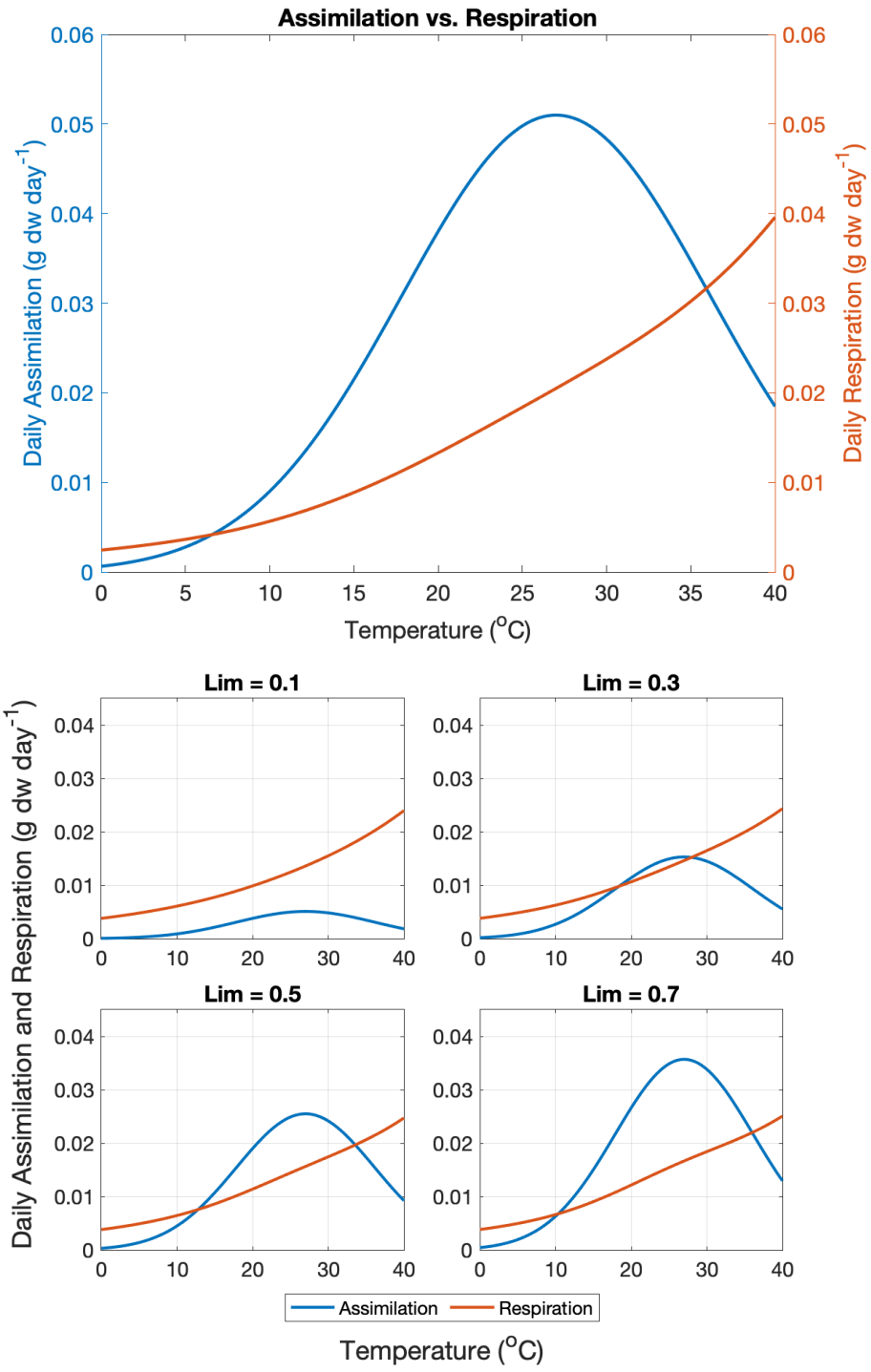

Figure S1. Daily assimilation and respiration rates of Eastern oysters as a function of temperature as simulated by the EcoOyster model. Rates are shown (a) assuming no limitation on filtration (Lim = 1) and (b) when filtration is limited by other environmental conditions. (Lim = a dimensionless product of limiting functions of salinity, TSS, dissolved oxygen, and chl*a*).

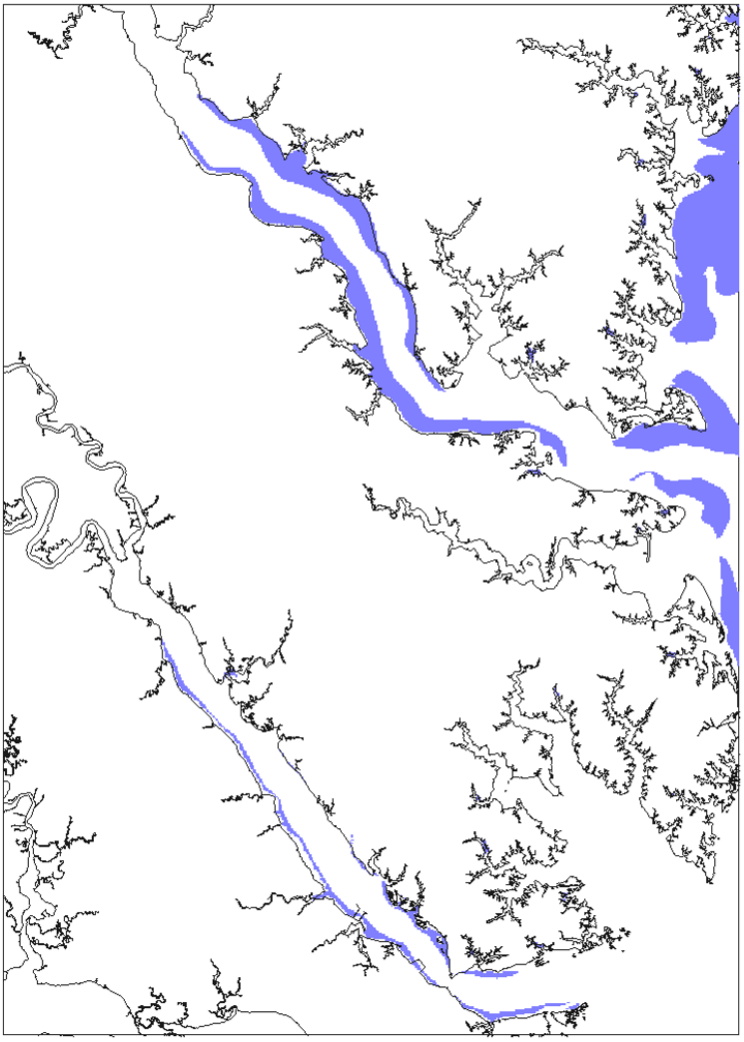

Figure S2. ROMS-ECBO model grid cells that support oyster growth (purple), defined as all grid cells where tissue weight in the reference run exceeds 1 g at the end of one year of growth.

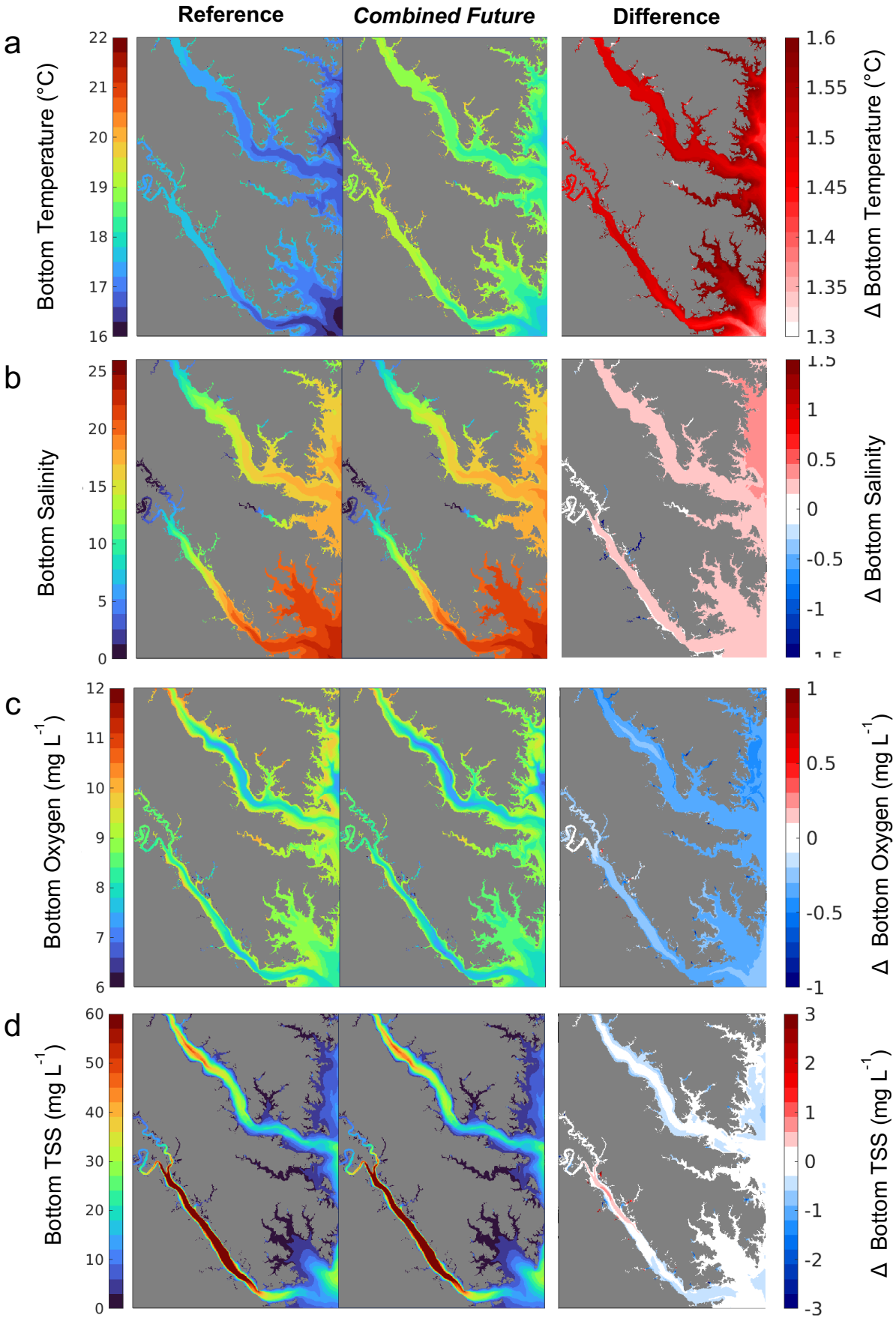

Figure S3. Annual mean bottom ROMS-ECBO bottom (a) temperature, (b) salinity, (c) O_2, and (d) TSS from the reference run, the *Combined Future* simulation, and *Combined Future* minus reference.

BIBLIOGRAPHY

Abatzoglou, J. T. and Brown, T. J.: A comparison of statistical downscaling methods suited for wildfire applications, Int. J. Clim., 32, 772–780, https://doi.org/10.1002/joc.2312, 2012.

Amaral, V., Cabral, H. N., & Bishop, M. J.: Effects of estuarine acidification on predator–prey interactions. Marine Ecology Progress Series, 445, 117-127, https://doi.org/10.3354/meps09487, 2012.

Barton, S. and Yvon-Durocher, G.: Quantifying the temperature dependence of growth rate in marine phytoplankton within and across species, Limnol. Oceanogr., 64, 2081–2091, https://doi.org/10.1002/lno.11170, 2019.

Beniash, E., Ivanina, A., Lieb, N., Kurochkin, I., and Sokolova, I.: Elevated level of carbon dioxide affects metabolism and shell formation in oysters Crassostrea virginica (Gmelin), Mar. Ecol. Prog. Ser., 419, 95–108, https://doi.org/10.3354/meps08841, 2010.

Bertolini, C., Brigolin, D., Porporato, E. M. D., Hattab, J., Pastres, R., and Tiscar, P. G.: Testing a Model of Pacific Oysters' (Crassostrea gigas) Growth in the Adriatic Sea: Implications for Aquaculture Spatial Planning, Sustainability, 13, 3309, https://doi.org/10.3390/su13063309, 2021.

Bhatt, G., Linker, L., Shenk, G., Bertani, I., Tian, R., Rigelman, J., Hinson, K., and Claggett, P.: Water quality impacts of climate change, land use, and population growth in the Chesapeake Bay watershed, JAWRA J. Am. Water Resour. Assoc., 59, 1313–1341, https://doi.org/10.1111/1752-1688.13144, 2023.

Borges, A. V. and Gypens, N.: Carbonate chemistry in the coastal zone responds more strongly to eutrophication than to ocean acidification, Limnology and Oceanography, 55, 346–353, https://doi.org/10.4319/lo.2010.55.1.0346, 2010.

Boulais, M., Chenevert, K. J., Demey, A. T., Darrow, E. S., Robison, M. R., Roberts, J. P., and Volety, A.: Oyster reproduction is compromised by acidification experienced seasonally in coastal regions, Sci. Rep., 7, 13276, https://doi.org/10.1038/s41598-017-13480-3, 2017.

Brianik, C. J. and Allam, B.: The need for more information on the resistance to biological and environmental stressors in triploid oysters, Aquaculture, 577, 739913, https://doi.org/10.1016/j.aquaculture.2023.739913, 2023.

Bukaveckas, P. A.: Carbon dynamics at the river–estuarine transition: a comparison among tributaries of Chesapeake Bay, Biogeosciences, 19, 4209–4226, https://doi.org/10.5194/bg-19-4209-2022, 2022.

Burford, M., Scarpa, J., Cook, B., and Hare, M.: Local adaptation of a marine invertebrate with a high dispersal potential: evidence from a reciprocal transplant experiment of the eastern oyster Crassostrea virginica, Mar. Ecol. Prog. Ser., 505, 161–175, https://doi.org/10.3354/meps10796, 2014.

Burge, C. A., Judah, L. R., Conquest, L. L., Griffin, F. J., Cheney, D. P., Suhrbier, A., Vadopalas, B., Olin, P. G., Renault, T., and Friedman, C. S.: Summer seed mortality of the pacific oyster, Crassostrea gigas (Thunberg) grown in Tomales Bay, California, USA: the influence of oyster stock, planting time, pathogens, and environmental stressors, Journal of Shellfish Research, https://doi.org/10.2983/0730-8000, 2007.

Cai, W., Feely, R. A., Testa, J. M., Li, M., Evans, W., Alin, S. R., Xu, Y.-Y., Pelletier, G., Ahmed, A., Greeley, D. J., Newton, J. A., and Bednaršek, N.: Natural and Anthropogenic Drivers of Acidification in Large Estuaries, Annual Review of Marine Science, https://doi.org/10.1146/annurev-marine-010419-011004, 2021.

Cai, W.J., Huang, W.-J., Luther, G. W., Pierrot, D., Li, M., Testa, J., Xue, M., Joesoef, A., Mann, R., Brodeur, J., Xu, Y.-Y., Chen, B., Hussain, N., Waldbusser, G. G., Cornwell, J., and Kemp, W. M.: Redox reactions and weak buffering capacity lead to acidification in the Chesapeake Bay, Nat. Commun., 8, 369, https://doi.org/10.1038/s41467-017-00417-7, 2017.

Cai, W.J., Xu, Y.-Y., Feely, R. A., Wanninkhof, R., Jönsson, B., Alin, S. R., Barbero, L., Cross, J. N., Azetsu-Scott, K., Fassbender, A. J., Carter, B. R., Jiang, L.-Q., Pepin, P., Chen, B., Hussain, N., Reimer, J. J., Xue, L., Salisbury, J. E., Hernández-Ayón, J. M., Langdon, C., Li, Q., Sutton, A. J., Chen, C.-T. A., and Gledhill, D. K.: Controls on surface water carbonate chemistry along North American ocean margins, Nat. Commun., 11, 2691, https://doi.org/10.1038/s41467-020-16530-z, 2020.

Cai, W. J., & Wang, Y.: The chemistry, fluxes, and sources of carbon dioxide in the estuarine waters of the Satilla and Altamaha Rivers, Georgia. Limnology and Oceanography, 43(4), 657-668, https://doi.org/10.4319/lo.1998.43.4.0657, 1998.

Caldeira, K. and Wickett, M. E.: Anthropogenic carbon and ocean pH, Nature, 425, 365–365, https://doi.org/10.1038/425365a, 2003.

Caldeira, K. and Wickett, M. E.: Ocean model predictions of chemistry changes from carbon dioxide emissions to the atmosphere and ocean, J. Geophys. Res.: Oceans, 110, https://doi.org/10.1029/2004jc002671, 2005.

Callam, B. R., Allen, S. K., and Frank-Lawale, A.: Genetic and environmental influence on triploid Crassostrea virginica grown in Chesapeake Bay: Growth, Aquaculture, 452, 97–106, https://doi.org/10.1016/j.aquaculture.2015.10.027, 2016.

Carstensen, J. and Duarte, C. M.: Drivers of pH Variability in Coastal Ecosystems, Environ. Sci. Technol., 53, 4020–4029, https://doi.org/10.1021/acs.est.8b03655, 2019.

Cerco, C. and Noel, M.: Process-based primary production modeling in Chesapeake Bay, Mar. Ecol. Prog. Ser., 282, 45–58, https://doi.org/10.3354/meps282045, 2004.

Cerco, C. F. and Noel, M. R.: Nonnative Oysters in the Chesapeake Bay, 2005.

Cerco, C. F., Noel, M. R., and Wang, P.: The Shallow-Water Component of the Chesapeake Bay Environmental Model Package, JAWRA J. Am. Water Resour. Assoc., 49, 1091–1102, https://doi.org/10.1111/jawr.12106, 2013.

Chesapeake Bay Program DataHub: https://datahub.chesapeakebay.net/, last access: 28 January 2024

Comeau, L. A., Mayrand, É., and Mallet, A.: Winter quiescence and spring awakening of the Eastern oyster Crassostrea virginica at its northernmost distribution limit, Mar. Biol., 159, 2269–2279, https://doi.org/10.1007/s00227-012-2012-8, 2012.

Copernicus Climate Change Service: ERA5: Fifth Generation of ECMWF Atmospheric Reanalyses of the Global Climate, Copernicus Climate Change Service Climate Data Store (CDS). https://cds.climate.copernicus.eu/cdsapp#!/home, 2017.

Da, F., Friedrichs, M. A. M., St-Laurent, P., Shadwick, E. H., Najjar, R. G., and Hinson, K. E.: Mechanisms Driving Decadal Changes in the Carbonate System of a Coastal Plain Estuary, J. Geophys. Res.: Oceans, 126, https://doi.org/10.1029/2021jc017239, 2021.

Da, F: Chesapeake Bay Carbon Cycle: Past, Present, Future, PhD. Dissertation, Virginia Institute of Marine Science, William & Mary, Virginia, USA, https://dx.doi.org/10.25773/v5-46f7-e286, 2023.

Dégremont, L., Garcia, C., Frank-Lawale, A., and Allen, S. K.: Triploid Oysters in the Chesapeake Bay: Comparison of Diploid and Triploid Crassostrea virginica, J. Shellfish Res., 31, 21–31, https://doi.org/10.2983/035.031.0103, 2012.

Dickinson, G. H., Ivanina, A. V., Matoo, O. B., Pörtner, H. O., Lannig, G., Bock, C., Beniash, E., and Sokolova, I. M.: Interactive effects of salinity and elevated CO2 levels on juvenile eastern oysters, Crassostrea virginica, J. Exp. Biol., 215, 29–43, https://doi.org/10.1242/jeb.061481, 2011.

Doney, S. C., Fabry, V. J., Feely, R. A., and Kleypas, J. A.: Ocean acidification: the other CO_2 problem., Annu. Rev. Mar. Sci., 1, 169–92, https://doi.org/10.1146/annurev.marine.010908.163834, 2009.

Dong, S., Lei, Y., Li, T., Cao, Y., & Xu, K.: Biocalcification crisis in the continental shelf under ocean acidification. Geoscience Frontiers, 14(6), 101622, https://doi.org/10.1016/j.gsf.2023.101622, 2023.

Du, J., Shen, J., Park, K., Wang, Y. P., and Yu, X.: Worsened physical condition due to climate change contributes to the increasing hypoxia in Chesapeake Bay, Sci. Total Environ., 630, 707–717, https://doi.org/10.1016/j.scitotenv.2018.02.265, 2018.

Duarte, C. M., Hendriks, I. E., Moore, T. S., Olsen, Y. S., Steckbauer, A., Ramajo, L., Carstensen, J., Trotter, J. A., and McCulloch, M.: Is Ocean Acidification an Open-Ocean Syndrome? Understanding Anthropogenic Impacts on Seawater pH, Estuaries Coasts, 36, 221–236, https://doi.org/10.1007/s12237-013-9594-3, 2013.

Dufresne, J.-L., Foujols, M.-A., Denvil, S., Caubel, A., Marti, O., Aumont, O., Balkanski, Y., Bekki, S., Bellenger, H., Benshila, R., Bony, S., Bopp, L., Braconnot, P., Brockmann, P., Cadule, P., Cheruy, F., Codron, F., Cozic, A., Cugnet, D., Noblet, N. de, Duvel, J.-P., Ethé, C., Fairhead, L., Fichefet, T., Flavoni, S., Friedlingstein, P., Grandpeix, J.-Y., Guez, L., Guilyardi, E., Hauglustaine, D., Hourdin, F., Idelkadi, A., Ghattas, J., Joussaume, S., Kageyama, M., Krinner, G., Labetoulle, S., Lahellec, A., Lefebvre, M.-P., Lefevre, F., Levy, C., Li, Z. X., Lloyd, J., Lott, F., Madec, G., Mancip, M., Marchand, M., Masson, S., Meurdesoif, Y., Mignot, J., Musat, I., Parouty, S., Polcher, J., Rio, C., Schulz, M., Swingedouw, D., Szopa, S., Talandier, C., Terray, P., Viovy, N., and Vuichard, N.: Climate change projections using the IPSL-CM5 Earth System Model: from CMIP3 to CMIP5, Clim. Dyn., 40, 2123–2165, https://doi.org/10.1007/s00382-012-1636-1, 2013.

Dunne, J. P., John, J. G., Adcroft, A. J., Griffies, S. M., Hallberg, R. W., Shevliakova, E., Stouffer, R. J., Cooke, W., Dunne, K. A., Harrison, M. J., Krasting, J. P., Malyshev, S. L., Milly, P. C. D., Phillipps, P. J., Sentman, L. T., Samuels, B. L., Spelman, M. J., Winton, M., Wittenberg, A. T., and Zadeh, N.: GFDL's ESM2 Global Coupled Climate–Carbon Earth System Models. Part I: Physical Formulation and Baseline Simulation Characteristics, J. Clim., 25, 6646–6665, https://doi.org/10.1175/jcli-d-11-00560.1, 2012.

EPA, Chesapeake Bay Total Maximum Daily Load for Nitrogen, Phosphorus, and Sediment, United States Environmental Protection Agency, 2010.
Guinotte, J. M. and Fabry, V. J.: Ocean Acidification and Its Potential Effects on Marine Ecosystems, Ann. N. York Acad. Sci., 1134, 320–342, https://doi.org/10.1196/annals.1439.013, 2008.

Ehrich, M. K. and Harris, L. A.: A review of existing eastern oyster filtration rate models, Ecol. Model., 297, 201–212, https://doi.org/10.1016/j.ecolmodel.2014.11.023, 2015.

Feely, R. A., Sabine, C. L., Lee, K., Berelson, W., Kleypas, J., Fabry, V. J., and Millero, F. J.: Impact of Anthropogenic CO2 on the CaCO3 System in the Oceans, Science Magazine, 305, 362–366, https://doi.org/10.1126/science.1097329, 2004.

Feely, R. A., Doney, S. C., and Cooley, S. R.: Ocean Acidification: Present Conditions and Future Changes in a High-CO_2 World, Oceanography, 22, 36–47, https://doi.org/10.5670/oceanog.2009.95, 2009.

Feng, Y., Friedrichs, M. A. M., Wilkin, J., Tian, H., Yang, Q., Hofmann, E. E., Wiggert, J. D., and Hood, R. R.: Chesapeake Bay nitrogen fluxes derived from a land-estuarine ocean biogeochemical modeling system: Model description, evaluation, and nitrogen budgets, J. Geophys. Res.: Biogeosciences, 120, 1666–1695, https://doi.org/10.1002/2015jg002931, 2015.

Fitzer, S. C., Torres Gabarda, S., Daly, L., Hughes, B., Dove, M., O'Connor, W., Potts, J., Scanes, P., & Byrne, M.: Coastal acidification impacts on shell mineral structure of bivalve mollusks. Ecology and evolution, 8(17), 8973-8984, https://doi.org/10.1002/ece3.4416, 2018.

Frankel, L. T., Friedrichs, M. A. M., St-Laurent, P., Bever, A. J., Lipcius, R. N., Bhatt, G., and Shenk, G. W.: Nitrogen reductions have decreased hypoxia in the Chesapeake Bay: Evidence from empirical and numerical modeling, Sci. Total Environ., 814, 152722, https://doi.org/10.1016/j.scitotenv.2021.152722, 2022.

Frank-Lawale, A., Allen, S. K., and Dgremont, L.: Breeding and Domestication of Eastern Oyster (Crassostrea virginica) Lines for Culture in the Mid-Atlantic, Usa: Line Development and Mass Selection for Disease Resistance, J. Shellfish Res., 33, 153–165, https://doi.org/10.2983/035.033.0115, 2014.

Fujii, M., Hamanoue, R., Bernardo, L. P. C., Ono, T., Dazai, A., Oomoto, S., Wakita, M., and Tanaka, T.: Assessing impacts of coastal warming, acidification, and deoxygenation on Pacific oyster (Crassostrea gigas) farming: a case study in the Hinase area, Okayama Prefecture, and Shizugawa Bay, Miyagi Prefecture, Japan, Biogeosciences, 20, 4527–4549, https://doi.org/10.5194/bg-20-4527-2023, 2023.

Fulford, R., Breitburg, D., Newell, R., Kemp, W., and Luckenbach, M.: Effects of oyster population restoration strategies on phytoplankton biomass in Chesapeake Bay: a flexible modeling approach, Mar. Ecol. Prog. Ser., 336, 43–61, https://doi.org/10.3354/meps336043, 2007.

Gattuso, Strong, A. L., Kroeker, K. J., Teneva, L. T., Mease, L. A., and Kelly, R. P.: Ocean Acidification 2.0: Managing our Changing Coastal Ocean Chemistry, BioScience, 64, 581–592, https://doi.org/10.1093/biosci/biu072, 2014.

Gazeau, F., Quiblier, C., Jansen, J. M., Gattuso, J. P., Middelburg, J. J., & Heip, C. H.: Impact of elevated CO_2 on shellfish calcification. Geophysical research letters, 34(7), https://doi.org/10.1029/2006GL028554, 2007.

Gobler, C. J. and Talmage, S. C.: Physiological response and resilience of early life-stage Eastern oysters (Crassostrea virginica) to past, present and future ocean acidification, Conserv. Physiol., 2, cou004, https://doi.org/10.1093/conphys/cou004, 2014.

Goulletquer, P., Soletchnik, P., Le Moine, O., Razet, D., Geairon, P., & Faury, N.: Summer mortality of the Pacific cupped oyster Crassostrea gigas in the Bay of Marennes-Oléron (France), *CIEM Conseil International pour l'Exploration de la Mer*, 1998.

Gruber, N., Clement, D., Carter, B. R., Feely, R. A., Heuven, S. van, Hoppema, M., Ishii, M., Key, R. M., Kozyr, A., Lauvset, S. K., Monaco, C. L., Mathis, J. T., Murata, A., Olsen, A., Perez, F. F., Sabine, C. L., Tanhua, T., and Wanninkhof, R.: The oceanic sink for anthropogenic CO2 from 1994 to 2007, Science, 363, 1193–1199, https://doi.org/10.1126/science.aau5153, 2019.

Gmelin, J. F.: Caroli a Linnaei Systema Naturae per Regna Tria Naturae, *Systema Naturae, Linneaeus, 13,* 3021-3910, 1791.

Guévélou, E., Carnegie, R. B., Small, J. M., Hudso n, K., Reece, K. S., and Rybovich, M. M.: Tracking Triploid Mortalities of Eastern Oysters Crassostrea virginica in the Virginia Portion of the Chesapeake Bay, J. Shellfish Res., 38, 101–113, https://doi.org/10.2983/035.038.0110, 2019.

Hasler, C. T., Jeffrey, J. D., Schneider, E. V. C., Hannan, K. D., Tix, J. A., and Suski, C. D.: Biological consequences of weak acidification caused by elevated carbon dioxide in freshwater ecosystems, Hydrobiologia, 806, 1–12, https://doi.org/10.1007/s10750-017-3332-y, 2018.

Herrmann, M., Najjar, R. G., Da, F., Friedman, J. R., Friedrichs, M. A. M., Goldberger, S., Menendez, A., Shadwick, E. H., Stets, E. G., and St-Laurent, P.: Challenges in Quantifying Air-Water Carbon Dioxide Flux Using Estuarine Water Quality Data: Case Study for Chesapeake Bay, J. Geophys. Res.: Oceans, 125, e2019JC015610, https://doi.org/10.1029/2019jc015610, 2020.

Hersbach, H., Bell, B., Berrisford, P., Hirahara, S., Horányi, A., Muñoz-Sabater, J., Nicolas, J., Peubey, C., Radu, R., Schepers, D., Simmons, A., Soci, C., Abdalla, S., Abellan, X., Balsamo, G., Bechtold, P., Biavati, G., Bidlot, J., Bonavita, M., Chiara, G., Dahlgren, P., Dee, D., Diamantakis, M., Dragani, R., Flemming, J., Forbes, R., Fuentes, M., Geer, A., Haimberger, L., Healy, S., Hogan, R. J., Hólm, E., Janisková, M., Keeley, S., Laloyaux, P., Lopez, P., Lupu, C., Radnoti, G., Rosnay, P., Rozum, I., Vamborg, F., Villaume, S., and Thépaut, J.: The ERA5 global reanalysis, Q. J. R. Meteorol. Soc., 146, 1999–2049, https://doi.org/10.1002/qj.3803, 2020.

Hinson, K. E., Friedrichs, M. A. M., St-Laurent, P., Da, F., and Najjar, R. G.: Extent and Causes of Chesapeake Bay Warming, JAWRA J. Am. Water Resour. Assoc., 58, 805–825, https://doi.org/10.1111/1752-1688.12916, 2022.

Hinson, K. E., Friedrichs, M. A. M., Najjar, R. G., Herrmann, M., Bian, Z., Bhatt, G., St-Laurent, P., Tian, H., and Shenk, G.: Impacts and uncertainties of climate-induced changes in watershed inputs on estuarine hypoxia, Biogeosciences, 20, 1937–1961, https://doi.org/10.5194/bg-20-1937-2023, 2023.

Hochachka, P. W. and Somero, G. N.: Biochemical Adaptation: Mechanism and Processing Physiological Evolution. Oxford University Press, 2002.

Hofmann, G. E. and Hand, S. C.: Global arrest of translation during invertebrate quiescence., Proc. Natl. Acad. Sci., 91, 8492–8496, https://doi.org/10.1073/pnas.91.18.8492, 1994.

Hopkinson, C. S., Buffam, I., Hobbie, J., Vallino, J., Perdue, M., Eversmeyer, B., Prahl, F., Covert, J., Hodson, R., Moran, M. A., Smith, E., Baross, J., Crump, B., Findlay, S., and Foreman, K.: Terrestrial inputs of organic matter to coastal ecosystems: An intercomparison of chemical characteristics and bioavailability, Biogeochemistry, 43, 211–234, https://doi.org/10.1023/a:1006016030299, 1998.

Hudson, K.: Virginia Shellfish Aquaculture Situation and Outlook Report:Results of the 2018 Virginia Shellfish Aquaculture Crop Reporting Survey, 2019.

Intergovernmental Panel on Climate Change: IPCC Special Report on the Ocean and Cryosphere in a Changing Climate [H.-O. Pörtner, D.C. Roberts, V. Masson-Delmotte, P. Zhai, M. Tignor, E. Poloczanska, K. Mintenbeck, A. Alegría, M. Nicolai, A. Okem, J. Petzold, B. Rama, N.M. Weyer (eds.)]. Cambridge University Press, Cambridge, UK and New York, NY, USA, 755 pp. https://doi.org/10.1017/9781009157964, 2019.

Intergovernmental Panel on Climate Change: The Physical Science Basis, 673–816, https://doi.org/10.1017/9781009157896.007, 2021.

Irby, I. D., Friedrichs, M. A. M., Friedrichs, C. T., Bever, A. J., Hood, R. R., Lanerolle, L. W. J., Li, M., Linker, L., Scully, M. E., Sellner, K., Shen, J., Testa, J., Wang, H., Wang, P., and Xia, M.: Challenges associated with modeling low-oxygen waters in Chesapeake Bay: a multiple model comparison, Biogeosciences, 13, 2011–2028, https://doi.org/10.5194/bg-13-2011-2016, 2016.

Irby, I. D., Friedrichs, M. A. M., Da, F., and Hinson, K. E.: The competing impacts of climate change and nutrient reductions on dissolved oxygen in Chesapeake Bay, Biogeosciences, 15, 2649–2668, https://doi.org/10.5194/bg-15-2649-2018, 2018.

Jewett, L. and Romanou, A: Ocean acidification and other ocean changes. In: Climate Science Special Report: Fourth National Climate Assessment, Volume I [Wuebbles, D.J., D.W. Fahey, K.A. Hibbard, D.J. Dokken, B.C. Stewart, and T.K. Maycock (eds.)]. U.S. Global Change Research Program, Washington, DC, USA, pp. 364-392, doi: 10.7930/J0QV3JQB, 2017.

Jones, H. R., Johnson, K. M., and Kelly, M. W.: Synergistic Effects of Temperature and Salinity on the Gene Expression and Physiology of Crassostrea virginica, Integr. Comp. Biol., 59, 306–319, https://doi.org/10.1093/icb/icz035, 2019.

Jordan, S. J.: Sedimentation and remineralization associated with biodeposition by the American oyster *Crassostrea virginica* (Gmelin). University of Maryland, College Park, 1987.

Kellogg, M. L., Brush, M., and Cornwell, J. C.: An updated model for estimating the TMDL-related benefits of oyster reef restoration, A final report to The Nature Conservancy and Oyster Recovery Partnership, 2018.

Kelly, C. J., Laramore, S. E., Scarpa, J., and Newell, R. I. E.: Seasonal Comparison of Physiological Adaptation and Growth of Suminoe (Crassostrea ariakensis) and Eastern (Crassostrea virginica) Oysters, J. Shellfish Res., 30, 737–749, https://doi.org/10.2983/035.030.0314, 2011.

Kemp, W., Boynton, W., Adolf, J., Boesch, D., Boicourt, W., Brush, G., Cornwell, J., Fisher, T., Glibert, P., Hagy, J., Harding, L., Houde, E., Kimmel, D., Miller, W., Newell, R., Roman, M., Smith, E., and Stevenson, J.: Eutrophication of Chesapeake Bay: historical trends and ecological interactions, Mar. Ecol. Prog. Ser., 303, 1–29, https://doi.org/10.3354/meps303001, 2005.

Kingsley-Smith, P. R., Harwell, H. D., Kellogg, M. L., Allen, S. M., Allen, S. K., Meritt, D. W., Paynter, K. T., and Luckenbach, M. W.: Survival and Growth of Triploid Crassostrea virginica (Gmelin, 1791) and C. ariakensis (Fujita, 1913) in Bottom Environments of Chesapeake Bay: Implications for an Introduction, J. Shellfish Res., 28, 169–184, https://doi.org/10.2983/035.028.0201, 2009.

Lake, S. and Brush, M.: Modeling estuarine response to load reductions in a warmer climate: York River Estuary, Virginia, USA, Mar. Ecol. Prog. Ser., 538, 81–98, https://doi.org/10.3354/meps11448, 2015.

Lavaud, R., Peyre, M. K. L., Justic, D., and Peyre, J. F. L.: Dynamic Energy Budget modelling to predict eastern oyster growth, reproduction, and mortality under river management and climate change scenarios, Estuar., Coast. Shelf Sci., 251, 107188, https://doi.org/10.1016/j.ecss.2021.107188, 2021.

Lavaud, R., Peyre, M. K. L., Couvillion, B., Pollack, J. B., Brown, V., Palmer, T. A., and Keim, B.: Predicting restoration and aquaculture potential of eastern oysters through an eco-physiological mechanistic model, Ecol. Model., 489, 110603, https://doi.org/10.1016/j.ecolmodel.2023.110603, 2024.

Lemasson, A. J., Hall-Spencer, J. M., Fletcher, S., Provstgaard-Morys, S., and Knights, A. M.: Indications of future performance of native and non-native adult oysters under acidification and warming, Mar. Environ. Res., 142, 178–189, https://doi.org/10.1016/j.marenvres.2018.10.003, 2018.

Li, M., Lee, Y. J., Testa, J. M., Li, Y., Ni, W., Kemp, W. M., and Toro, D. M. D.: What drives interannual variability of hypoxia in Chesapeake Bay: Climate forcing versus nutrient loading?, Geophys. Res. Lett., 43, 2127–2134, https://doi.org/10.1002/2015gl067334, 2016.

Liddel, M. K.: A von Bertalanffy based model for the estimation of oyster (Crassostrea virginica) growth on restored oyster reefs in Chesapeake Bay, 2008.

Liu, Z., Zhou, Z., Zhang, Y., Wang, L., Song, X., Wang, W., ... & Song, L.: Ocean acidification inhibits initial shell formation of oyster larvae by suppressing the biosynthesis of serotonin and dopamine. Science of The Total Environment, 735, 139469, https://doi.org/10.1016/j.scitotenv.2020.139469, 2020

Loosanoff, V. L.: some aspects of behavior of oysters at different temperatures, Biol. Bull., 114, 57–70, https://doi.org/10.2307/1538965, 1958.

Loosanoff, V. L. And nomejko, c. A.: growth of oysters, o. Virginica, during different months, Biol. Bull., 97, 82–94, https://doi.org/10.2307/1538096, 1949.

López-Urrutia, Á., Martin, E. S., Harris, R. P., and Irigoien, X.: Scaling the metabolic balance of the oceans, Proc. Natl. Acad. Sci., 103, 8739–8744, https://doi.org/10.1073/pnas.0601137103, 2006.

Lowe, A. T., Kobelt, J., Horwith, M., and Ruesink, J.: Ability of Eelgrass to Alter Oyster Growth and Physiology Is Spatially Limited and Offset by Increasing Predation Risk, Estuaries Coasts, 42, 743–754, https://doi.org/10.1007/s12237-018-00488-9, 2019.

Lutier, M., Di Poi, C., Gazeau, F., Appolis, A., Le Luyer, J., & Pernet, F.: Revisiting tolerance to ocean acidification: insights from a new framework combining physiological and molecular tipping points of Pacific oyster. *Global change biology*, *28*(10), 3333-3348, https://doi.org/10.1111/gcb.16101, 2022

Mazarrasa, I., Marbà, N., Lovelock, C. E., Serrano, O., Lavery, P. S., Fourqurean, J. W., Kennedy, H., Mateo, M. A., Krause-Jensen, D., Steven, A. D. L., and Duarte, C. M.: Seagrass meadows as a globally significant carbonate reservoir, Biogeosciences, 12, 4993–5003, https://doi.org/10.5194/bg-12-4993-2015, 2015.

Matoo, O. B., Lannig, G., Bock, C., & Sokolova, I. M.: Temperature but not ocean acidification affects energy metabolism and enzyme activities in the blue mussel, Mytilus edulis. *Ecology and evolution*, *11*(7), 3366-3379, https://doi.org/10.1002/ece3.7289, 2021.

Medeiros, I. P. M., & Souza, M. M.: Acid times in physiology: a systematic review of the effects of ocean acidification on calcifying invertebrates. *Environmental Research*, 116019, https://doi.org/10.1016/j.envres.2023.116019, 2023

Melzner, F., Mark, F.C., Seibel, B.A. and Tomanek, L.: Ocean acidification and coastal marine invertebrates: tracking CO2 effects from seawater to the cell. *Annual Review of Marine Science*, *12*, pp.499-523, https://doi.org/10.1146/annurev-marine-010419-010658, 2020.

Mitchell, M., Herman, J., Bilkovic, D. M., and Hershner, C.: Marsh persistence under sea-level rise is controlled by multiple, geologically variable stressors, Ecosyst. Heal. Sustain., 3, 1379888, https://doi.org/10.1080/20964129.2017.1396009, 2017.

Mizuta, D. D., Silveira, N., Fischer, C. E., and Lemos, D.: Interannual variation in commercial oyster (Crassostrea gigas) farming in the sea (Florianópolis, Brazil, 27°44′ S; 48°33′ W) in relation to temperature, chlorophyll a and associated oceanographic conditions, Aquaculture, 366, 105–114, https://doi.org/10.1016/j.aquaculture.2012.09.011, 2012.

Mizuta, D. D. and Wikfors, G. H.: Seeking the perfect oyster shell: a brief review of current knowledge, Rev. Aquac., 11, 586–602, https://doi.org/10.1111/raq.12247, 2019.

Moore, K. A., Orth, R. J., and Wilcox, D. J.: Assessment of the Abundance of Submersed Aquatic Vegetation (SAV) Communities in the Chesapeake Bay and its Use in SAV Management, in: Remote Sensing and Geospatial Technologies for Coastal Ecosystem Assessment and Management, https://doi.org/10.1007/978-3-540-88183-4, 2009.

Moore-Maley, B. L., Allen, S. E., and Ianson, D.: Locally driven interannual variability of near-surface pH and ΩA in the Strait of Georgia, J. Geophys. Res.: Oceans, 121, 1600–1625, https://doi.org/10.1002/2015jc011118, 2016.

Moriarty, J. M., Friedrichs, M. A. M., and Harris, C. K.: Seabed Resuspension in the Chesapeake Bay: Implications for Biogeochemical Cycling and Hypoxia, Estuaries Coasts, 44, 103–122, https://doi.org/10.1007/s12237-020-00763-8, 2021.

Najjar, R. G., Herrmann, M., Valle, S. M. C. D., Friedman, J. R., Friedrichs, M. A. M., Harris, L. A., Shadwick, E. H., Stets, E. G., and Woodland, R. J.: Alkalinity in Tidal Tributaries of the Chesapeake Bay, J. Geophys. Res.: Oceans, 125, https://doi.org/10.1029/2019jc015597, 2020.

Newell, R. I. E. and Koch, E. W.: Modeling seagrass density and distribution in response to changes in turbidity stemming from bivalve filtration and seagrass sediment stabilization, Estuaries, 27, 793–806, https://doi.org/10.1007/bf02912041, 2004.

Ni, W., Li, M., and Testa, J. M.: Discerning effects of warming, sea level rise and nutrient management on long-term hypoxia trends in Chesapeake Bay, Sci. Total Environ., 737, 139717, https://doi.org/10.1016/j.scitotenv.2020.139717, 2020.

Olson, M.: Guide to Using Chesapeake Bay Program Water Quality Monitoring Data, Chesapeake Bay Program, Annapolis, MD, 2012.

Orth, R. J., Nowak, J. F., Wilcox, D. J., Whiting, J. R., and Nagey, L. S.: Distribution of Submerged Aquatic Vegetation in the Chesapeake Bay and Tributaries and the Coastal Bays - 1998, Am. Zoöl., 3, 315–317, https://doi.org/10.1093/icb/3.3.315, 199AD.

Palmer, S. C. J., Gernez, P. M., Thomas, Y., Simis, S., Miller, P. I., Glize, P., and Barillé, L.: Remote Sensing-Driven Pacific Oyster (Crassostrea gigas) Growth Modeling to Inform Offshore Aquaculture Site Selection, Front. Mar. Sci., 6, 802, https://doi.org/10.3389/fmars.2019.00802, 2020.

Palmer, S. C. J., Barillé, L., Kay, S., Ciavatta, S., Buck, B., and Gernez, P.: Pacific oyster (Crassostrea gigas) growth modelling and indicators for offshore aquaculture in Europe under climate change uncertainty, Aquaculture, 532, 736116, https://doi.org/10.1016/j.aquaculture.2020.736116, 2021.

Paynter, K. T., Goodwin, J. D., Chen, M. E., Ward, N. J., Sherman, M. W., Meritt, D. W., and Allen, S. K.: *Crassostrea ariakensis* in Chesapeake Bay: Growth, Disease and Mortality in

Shallow Subtidal Environments, J. Shellfish Res., 27, 509–515, https://doi.org/10.2983/0730-8000(2008)27[509:caicbg]2.0.co;2, 2008.

Peyre, M. K. L., Eberline, B. S., Soniat, T. M., and Peyre, J. F. L.: Differences in extreme low salinity timing and duration differentially affect eastern oyster (Crassostrea virginica) size class growth and mortality in Breton Sound, LA, Estuar., Coast. Shelf Sci., 135, 146–157, https://doi.org/10.1016/j.ecss.2013.10.001, 2013.

Planton, S., Déqué, M., Chauvin, F., and Terray, L.: Expected impacts of climate change on extreme climate events, C. R. Geosci., 340, 564–574, https://doi.org/10.1016/j.crte.2008.07.009, 2008.

Ramajo, L., Pérez-León, E., Hendriks, I. E., Marbà, N., Krause-Jensen, D., Sejr, M. K., Blicher, M. E., Lagos, N. A., Olsen, Y. S., and Duarte, C. M.: Food supply confers calcifiers resistance to ocean acidification, Sci. Rep., 6, 19374, https://doi.org/10.1038/srep19374, 2016.

Raymond, P. A., Bauer, J. E., and Cole, J. J.: Atmospheric CO2 evasion, dissolved inorganic carbon production, and net heterotrophy in the York River estuary, Limnol. Oceanogr., 45, 1707–1717, https://doi.org/10.4319/lo.2000.45.8.1707, 2000.

Riahi, K., Rao, S., Krey, V., Cho, C., Chirkov, V., Fischer, G., Kindermann, G., Nakicenovic, N., and Rafaj, P.: RCP 8.5—A scenario of comparatively high greenhouse gas emissions, Clim. Chang., 109, 33, https://doi.org/10.1007/s10584-011-0149-y, 2011.

Rivest, E.B. , Brush, M., Zimmerman, R., Hill., V," Can Meadows of Submerged Aquatic Vegetation (SAV) Mitigate Ocean Acidification Thresholds for Eastern Oysters in the Chesapeake Bay? Final report, NOAA Ocean Acidification Program. Award number NA18NOS4780177, 2023.

Roden, E. and Tuttle, J.: Inorganic sulfur cycling in mid and lower Chesapeake Bay sediments, Mar. Ecol. Prog. Ser., 93, 101–118, https://doi.org/10.3354/meps093101, 1993.

Rybovich, M., Peyre, M. K. L., Hall, S. G., and Peyre, J. F. L.: Increased Temperatures Combined with Lowered Salinities Differentially Impact Oyster Size Class Growth and Mortality, J. Shellfish Res., 35, 101–113, https://doi.org/10.2983/035.035.0112, 2016.

Salisbury, J., Green, M., Hunt, C., and Campbell, J.: Coastal Acidification by Rivers: A Threat to Shellfish?, Eos, Trans. Am. Geophys. Union, 89, 513–513, https://doi.org/10.1029/2008eo500001, 2008.

Schwaner, C., Barbosa, M., Schwemmer, T. G., Espinosa, E. P., and Allam, B.: Increased Food Resources Help Eastern Oyster Mitigate the Negative Impacts of Coastal Acidification, Animals, 13, 1161, https://doi.org/10.3390/ani13071161, 2023.

Simone, M. N., Schulz, K. G., Oakes, J. M., and Eyre, B. D.: Warming and ocean acidification may decrease estuarine dissolved organic carbon export to the ocean, Biogeosciences, 18, 1823–1838, https://doi.org/10.5194/bg-18-1823-2021, 2021.

Nixon, S.W.: Coastal marine eutrophication: A definition, social causes, and future concerns, Ophelia, 41, 199-219, htpps://doi.org/10.1080/00785236.1995.10422044, 1995.

Shadwick, E. H., Friedrichs, M. A. M., Najjar, R. G., Meo, O. A. D., Friedman, J. R., Da, F., and Reay, W. G.: High-Frequency CO2 System Variability Over the Winter-to-Spring Transition in a Coastal Plain Estuary, J. Geophys. Res.: Oceans, 124, 7626–7642, https://doi.org/10.1029/2019jc015246, 2019.

Shchepetkin, A. F. and McWilliams, J. C.: The regional oceanic modeling system (ROMS): a split-explicit, free-surface, topography-following-coordinate oceanic model, Ocean Model., 9, 347–404, https://doi.org/10.1016/j.ocemod.2004.08.002, 2005.

Shen, C., Testa, J. M., Li, M., Cai, W., Waldbusser, G. G., Ni, W., Kemp, W. M., Cornwell, J., Chen, B., Brodeur, J., and Su, J.: Controls on Carbonate System Dynamics in a Coastal Plain Estuary: A Modeling Study, J. Geophys. Res.: Biogeosciences, 124, 61–78, https://doi.org/10.1029/2018jg004802, 2019a.

Shen, C., Testa, J. M., Ni, W., Cai, W., Li, M., and Kemp, W. M.: Ecosystem Metabolism and Carbon Balance in Chesapeake Bay: A 30-Year Analysis Using a Coupled Hydrodynamic-Biogeochemical Model, J. Geophys. Res.: Oceans, 124, 6141–6153, https://doi.org/10.1029/2019jc015296, 2019b.

Shen, C., Testa, J. M., Li, M., and Cai, W.: Understanding Anthropogenic Impacts on pH and Aragonite Saturation State in Chesapeake Bay: Insights From a 30-Year Model Study, J. Geophys. Res.: Biogeosciences, 125, https://doi.org/10.1029/2019jg005620, 2020.

Siedlecki, S., Salisbury, J., Gledhill, D., Bastidas, C., Meseck, S., McGarry, K., Hunt, C., Alexander, M., Lavoie, D., Wang, Z., Scott, J., Brady, D., Mlsna, I., Azetsu-Scott, K., Liberti, C., Melrose, D., White, M., Pershing, A., Vandemark, D., Townsend, D., Chen, C., Mook, W., and Morrison, R.: Projecting ocean acidification impacts for the Gulf of Maine to 2050, Elem.: Sci. Anthr., 9, https://doi.org/10.1525/elementa.2020.00062, 2021a.

Siedlecki, S. A., Pilcher, D., Howard, E. M., Deutsch, C., MacCready, P., Norton, E. L., Frenzel, H., Newton, J., Feely, R. A., Alin, S. R., and Klinger, T.: Coastal processes modify projections of some climate-driven stressors in the California Current System, Biogeosciences, 18, 2871–2890, https://doi.org/10.5194/bg-18-2871-2021, 2021b.

Speights, C. J., Silliman, B. R., and McCoy, M. W.: The effects of elevated temperature and dissolved ρCO2 on a marine foundation species, Ecol. Evol., 7, 3808–3814, https://doi.org/10.1002/ece3.2969, 2017.

Stevens, A. and Gobler, C.: Interactive effects of acidification, hypoxia, and thermal stress on growth, respiration, and survival of four North Atlantic bivalves, Mar. Ecol. Prog. Ser., 604, 143–161, https://doi.org/10.3354/meps12725, 2018.

St-Laurent, P. and Friedrichs, M. A. M.: On the Sensitivity of Coastal Hypoxia to Its External Physical Forcings, J. Adv. Model. Earth Syst., 16, https://doi.org/10.1029/2023ms003845, 2024.

St-Laurent, P., Friedrichs, M. A. M., Najjar, R. G., Shadwick, E. H., Tian, H., and Yao, Y.: Relative impacts of global changes and regional watershed changes on the inorganic carbon balance of the Chesapeake Bay, Biogeosciences, 17, 3779–3796, https://doi.org/10.5194/bg-17-3779-2020, 2020.

Su, J., Cai, W.-J., Brodeur, J., Chen, B., Hussain, N., Yao, Y., Ni, C., Testa, J. M., Li, M., Xie, X., Ni, W., Scaboo, K. M., Xu, Y., Cornwell, J., Gurbisz, C., Owens, M. S., Waldbusser, G. G., Dai, M., and Kemp, W. M.: Chesapeake Bay acidification buffered by spatially decoupled carbonate mineral cycling, Nat. Geosci., 13, 441–447, https://doi.org/10.1038/s41561-020-0584-3, 2020.

Swam, L. M., Couvillion, B., Callam, B., Peyre, J. F. L., and Peyre, M. K. L.: Defining oyster resource zones across coastal Louisiana for restoration and aquaculture, Ocean Coast. Manag., 225, 106178, https://doi.org/10.1016/j.ocecoaman.2022.106178, 2022.

Talmage, S. C. and Gobler, C. J.: Effects of Elevated Temperature and Carbon Dioxide on the Growth and Survival of Larvae and Juveniles of Three Species of Northwest Atlantic Bivalves, PLoS ONE, 6, e26941, https://doi.org/10.1371/journal.pone.0026941, 2011.

Tian, R., Cerco, C. F., Bhatt, G., Linker, L. C., and Shenk, G. W.: Mechanisms Controlling Climate Warming Impact on the Occurrence of Hypoxia in Chesapeake Bay, JAWRA J. Am. Water Resour. Assoc., 58, 855–875, https://doi.org/10.1111/1752-1688.12907, 2022.

Thomsen, J., Haynert, K., Wegner, K. M., and Melzner, F.: Impact of seawater carbonate chemistry on the calcification of marine bivalves, Biogeosciences, 12, 4209–4220, https://doi.org/10.5194/bg-12-4209-2015, 2015.

Turner, J. S., St-Laurent, P., Friedrichs, M. A. M., and Friedrichs, C. T.: Effects of reduced shoreline erosion on Chesapeake Bay water clarity, Sci. Total Environ., 769, 145157, https://doi.org/10.1016/j.scitotenv.2021.145157, 2021.

van Heuven, S., D. Pierrot, J.W.B. Lewis, R.E., and Wallace, D.W.R.: MATLAB Program Developed for CO2 System Calculations. ORNL/CDIAC-105b. Carbon Dioxide Information Analysis Center, Oak Ridge National Laboratory, U.S. Department of Energy, Oak Ridge, Tennessee. https://doi.org/10.3334/CDIAC/otg.CO2SYS_MATLAB_v1.1, 2011.

VOSARA: https://cmap22.vims.edu/VOSARA/,last access: 28 January 2024.

Waldbusser, G. G., Voigt, E. P., Bergschneider, H., Green, M. A., and Newell, R. I. E.: Biocalcification in the Eastern Oyster (Crassostrea virginica) in Relation to Long-term Trends in Chesapeake Bay pH, Estuaries Coasts, 34, 221–231, https://doi.org/10.1007/s12237-010-9307-0, 2011.

Waldbusser, G. G., Hales, B., Langdon, C. J., Haley, B. A., Schrader, P., Brunner, E. L., Gray, M. W., Miller, C. A., and Gimenez, I.: Saturation-state sensitivity of marine bivalve larvae to ocean acidification, Nat. Clim. Chang., 5, 273–280, https://doi.org/10.1038/nclimate2479, 2015.

Wallace, R. B., Baumann, H., Grear, J. S., Aller, R. C., and Gobler, C. J.: Coastal ocean acidification: The other eutrophication problem, Estuar., Coast. Shelf Sci., 148, 1–13, https://doi.org/10.1016/j.ecss.2014.05.027, 2014.

Warner, J. C., Defne, Z., Haas, K., and Arango, H. G.: A wetting and drying scheme for ROMS, Comput. Geosci., 58, 54–61, https://doi.org/10.1016/j.cageo.2013.05.004, 2013.

Zhang, Q., Fisher, T. R., Trentacoste, E. M., Buchanan, C., Gustafson, A. B., Karrh, R., Murphy, R. R., Keisman, J., Wu, C., Tian, R., Testa, J. M., and Tango, P. J.: Nutrient limitation of phytoplankton in Chesapeake Bay: Development of an empirical approach for water-quality management, Water Res., 188, 116407, https://doi.org/10.1016/j.watres.2020.116407, 2021.